AWARD NUMBER: W81XWH-13-1-0293

TITLE: An MEG Investigation of Neural Biomarkers and Language in Nonverbal Children with Autism Spectrum Disorders

PRINCIPAL INVESTIGATOR: Susan Hepburn, PhD

CONTRACTING ORGANIZATION: University of Colorado – Denver
Aurora, CO 80045

REPORT DATE: November 2016

TYPE OF REPORT: Final

PREPARED FOR: U.S. Army Medical Research and Materiel Command
Fort Detrick, Maryland 21702-5012

DISTRIBUTION STATEMENT: Approved for Public Release;
Distribution Unlimited

The views, opinions and/or findings contained in this report are those of the author(s) and should not be construed as an official Department of the Army position, policy or decision unless so designated by other documentation.

REPORT DOCUMENTATION PAGE

Form Approved
OMB No. 0704-0188

Public reporting burden for this collection of information is estimated to average 1 hour per response, including the time for reviewing instructions, searching existing data sources, gathering and maintaining the data needed, and completing and reviewing this collection of information. Send comments regarding this burden estimate or any other aspect of this collection of information, including suggestions for reducing this burden to Department of Defense, Washington Headquarters Services, Directorate for Information Operations and Reports (0704-0188), 1215 Jefferson Davis Highway, Suite 1204, Arlington, VA 22202-4302. Respondents should be aware that notwithstanding any other provision of law, no person shall be subject to any penalty for failing to comply with a collection of information if it does not display a currently valid OMB control number. **PLEASE DO NOT RETURN YOUR FORM TO THE ABOVE ADDRESS.**

1. REPORT DATE	2. REPORT TYPE	3. DATES COVERED
November 2016	Final	09/01/13 – 08/31/16

4. TITLE AND SUBTITLE

An MEG Investigation of Neural Biomarkers and Language in Nonverbal Children with Autism Spectrum Disorders

5a. CONTRACT NUMBER

5b. GRANT NUMBER
W81XWH-13-1-0293

5c. PROGRAM ELEMENT NUMBER

6. AUTHOR(S)

Susan Hepburn, PhD & Kristina M. Legget, Ph.D.

E-Mail: Kristina.legget@ucdenver.edu

5d. PROJECT NUMBER

5e. TASK NUMBER

5f. WORK UNIT NUMBER

7. PERFORMING ORGANIZATION NAME(S) AND ADDRESS(ES)

University of Colorado – Denver;
Anschutz Medical Campus, BLDG 500,
Mail stop F-428, PO BOX 508
Aurora, CO 80045

8. PERFORMING ORGANIZATION REPORT NUMBER

9. SPONSORING / MONITORING AGENCY NAME(S) AND ADDRESS(ES)

U.S. Army Medical Research and Material Command
Fort Detrick, Maryland 21702-5012

10. SPONSOR/MONITOR'S ACRONYM(S)

11. SPONSOR/MONITOR'S REPORT NUMBER(S)

12. DISTRIBUTION / AVAILABILITY STATEMENT

Approved for Public Release; Distribution Unlimited

13. SUPPLEMENTARY NOTES

14. ABSTRACT

Nonverbal individuals with autism spectrum disorders (ASD) are currently underrepresented in neuroimaging studies of ASD, leaving a critical gap in the understanding of language processing in ASD. The proposed project endeavored to address the challenges involved in imaging nonverbal children by: a) assessing function that does not necessitate a verbal response via magnetoencephalography (MEG), b) including multiple pre-imaging training methods to increase participant comfort and cooperation, and c) applying motion correction techniques post-recording to minimize movement Thirty-nine met eligibility criteria and completed the phenotype battery (i.e., standardized assessment of cognition, language and autism symptom measures) and were included one of three study groups: ASD/Minimally Verbal (n = 14); ASD/Verbal (n = 21) and Control/No ASD or DD (n = 4). Participants were then invited to complete pre-training activities to prepare them for the MEG appointment, followed by a 2-hour imaging session. The completion rate of imaging appointments that provided usable data was very low, across all 3 groups, even after adding an additional year to data collection through a no-cost extension. Barriers and lessons learned through the study are described.

15. SUBJECT TERMS

None listed

16. SECURITY CLASSIFICATION OF:			17. LIMITATION OF ABSTRACT	18. NUMBER OF PAGES	19a. NAME OF RESPONSIBLE PERSON
a. REPORT	b. ABSTRACT	c. THIS PAGE			USAMRMC
Unclassified	Unclassified	Unclassified	Unclassified	44	19b. TELEPHONE NUMBER *(include area code)*

Table of Contents

Page

1. Introduction…….4
2. Keywords…….4
3. Accomplishments……..……..... 4
4. Impact……..……9
5. Changes/Problems...…….10
6. Products……..12
7. Participants & Other Collaborating Organizations…….12
8. Special Reporting Requirements…….13
9. Appendices……14

1. Introduction:

Nonverbal individuals with autism spectrum disorders (ASD) are currently underrepresented in neuroimaging studies of ASD, leaving a critical gap in the understanding of language processing in ASD. The proposed project aims to address this gap by implementing individualized desensitization protocols and motion correction techniques to engage youth with ASD of all levels of functioning in two passive tasks of auditory processing, conducted during magnetoencephalography (MEG). The first task is a simple 5-minute auditory task during which participants hear a series of white noise stimuli. The second task is a 15-minute language task (with brief breaks throughout), in which participants hear spoken words followed by pictures that either match (e.g., spoken word "lion", picture of a lion) or do not match (e.g., spoken word "lion", picture of a boat). If the participant training protocol and motion correction procedures prove to be effective, this study has the potential to provide three measures that have been implicated as biomarkers in ASD: synchronized brain activity in the gamma frequency range (30-80 Hz), the M100 evoked field, and the M400 evoked field. The working hypothesis is that behavioral interventions, pre-training and motion correction will result in reliable imaging data of both verbal and nonverbal youth with ASD thus contributing to the to the knowledge of underlying neurophysiology in language processing in ASD.

2. Keywords: autism, neuroimaging, minimally verbal, auditory processing, language processing, biomarker

3. Accomplishments:

Project Goals and Accomplishments

Here is the statement of work for the project, accompanied by summary of progress across the 3-year project period (September 2013 – August 2016):

Task 1. Approval of human subjects' protocol with Colorado Multiple Institution Review Board. Progress: Done. Application submitted 4 months prior to the award start date; renewed each project year. The protocol is now closed, given that the PI is no longer at UC-Denver (Dr. Hepburn took a professorship at Colorado State University in August of 2016; simultaneous to finishing the no-cost extension year).

Task 2. Assessment Preparation. (a) Purchase behavioral assessment supplies (i.e., full kit for some, additional recording sheets for those for which the laboratory already has access to main testing materials). (b) Train Professional Research Assistant (PRA) on administration of cognitive and behavioral measures .Complete inter-observer reliability calibration with Postdoctoral fellow on autism diagnostic measures. Progress: Done. Three PRAs (2 advanced graduate students and 1 postdoctoral fellow) were engaged in assessment sessions and all three completed training to reach research reliability on the Autism Diagnostic Observation Schedule within the first 6 months.

Task 3. Participant Recruitment/Enrollment. (a) Coordinate recruitment strategy with clinical colleagues and co-investigators. (b) Send out recruitment letters to patient database and various agencies such as local community centered boards (i.e., regional centers). (c) Train PRA/Postdoctoral fellow on eligibility screening and informed consent

process. (d) Begin participant screening, consenting/enrolling by third quarter of year 1. (e) Recruit 36 youth; 12 in each of 3 groups (ASD/Minimally verbal; ASD/Verbal; and Typical Controls). Progress: Done/Met recruitment goal for ASD groups, but not for controls.

Recruiting Youth with ASD: Due to difficulties engaging youth with ASD in the imaging experiments, we bolstered our recruitment efforts significantly in year 2 and applied for approval to extend the study into a third year via a no-cost extension. In addition to sending out mailings to families within our ASD Phenotype database in Dr. Hepburn's lab at JFK Partners (the University Center for Excellence in Developmental Disabilities for Colorado), we also initiated a series of community-based workshops that we provided at no cost to families of youth with ASD. We covered topics that were reported to us to be relevant and interesting through a survey of the families in our research pool, including: *Toilet training Older Youth with ASD*, *Community Safety for Less Verbal Youth with ASD*, *Coping Skills for Youth with ASD* (2 workshops: 1 for less verbal and 1 for more verbal participants). At the end of the presentation, we shared information about current studies at the University of Colorado and emphasized the relevance of this particular study – especially for families of minimally verbal youth. In Years 2 & 3, Dr. Hepburn presented 9 community workshops in Colorado, extending to the mountain communities and to Wyoming in an effort to reach a wider constituency. 122 families provided their contact information and requested information about this study. We followed up by mailing the IRB-approved study announcement. Thirty-one parents then called the project to learn more and to complete the eligibility screening. This recruitment strategy resulted in the recruitment of 8 participants in year 2 and 11 in year 3. Word-of-mouth and responses to mailings also contributed to meeting the recruitment goal by bringing in 7 participants in year 2 and 6 in year 3.

Recruiting Typical Controls: We collaborated with our colleagues at the University of Denver and within our regional multi-institution research group – the Developmental Psychopathology Research Group – to send study announcements to Participant Pools developed to recruit healthy controls. These efforts resulted in just 16 inquiries from families; 8 did not meet eligibility criteria, as they were siblings of probands, 4 chose not to participate and 4 consented to participate. Next Steps: Investigators at UC-Denver continue to discuss strategies for recruiting healthy controls into imaging studies. Increasing the incentives to participate is one strategy that may have resulted in improved recruitment rates. We tried to extend the age range and engage young college students as controls; an approach that may have worked had we implemented it earlier in the project.

Task 4: Complete deep phenotyping battery on participants in the ASD groups. (a) When ADOS information is not already available for participants in autism groups, the autism diagnostic evaluations will be conducted by Dr. Hepburn and her staff. Inter-observer reliability on ADOS will be established and maintained at or above 85% (algorithm scores) on 40% of the sample. (b) Standardized assessments of cognitive, language and adaptive behaviors will be completed on all participants. (c) Formal reports that summarize standardized assessments will be sent to participating families, in part as an incentive for study engagement. Progress: Done. The team administered the ADOS to 30 youth across the study period. Inter-observer reliability on ADOS

algorithm scores was completed for 16 participants (more than 50%). Kappas ranged from .62-.84 across pairs of examiners, suggesting strong inter-observer reliability. Standardized assessments of cognition, language and adaptive behaviors were completed on 31 youth; followed by summary reports provided to their parents. Please see Table 1 for a summary of participant demographics and behavioral data.

Task 5. Preparing for Neuroimaging Visits. (a) For eligible participants, videos and other informational supports will be sent to parents to familiarize participants with imaging procedures. (b) Complete an Initial lab visit for consenting, behavioral measures, tour of imaging area. (c) For participants who show some hesitancy: Complete 2-4 additional visits to practice/become accustomed to the sound and experiences of being in the imaging machine.

Progress: Done. The team created a short film to show potential participants what its like to be in the MEG machine. The 8-minute movie depicts Will, a 15 year old with ASD and some language, coming to the lab, completing the MEG experiments, and earning a reinforcer for his efforts at the end. We mailed each enrolled family a USB containing the short film and a printable social story (created in powerpoint and attached in the appendices) and requested that they show one or both of these items to their son/daughter. During their first visit to the lab, we asked if they had watched the film or looked at the social story. Results: Of the 14 youth with ASD/Minimally verbal, 11 showed the film to the youth and 4 reported that the youth appeared interested. None of the parents of minimally verbal youth reported that their son/daughter watched the entire film, thus suggesting that the movie had limited salience to this subgroup. The social story was reported to be more useful by the parents of minimally verbal youth: all 14 parents showed the story at least once to their son/daughter prior to the appointment; 6 reported looking at it together more than once; 2 printed it out and read it multiple times. One family requested that we use photos of their son, which we did, resulting in more interest from him in looking at the story. Interestingly, all 4 of the minimally verbal youth who successfully completed the imaging experiments reviewed the social story with a parent more than one time before the imaging appointment.

Of the 21 youth with ASD who are verbal, the film was preferred over the social story by 17 (4 did not respond to the survey). These youth provided comments on the usefulness of the film and the majority rated it as “moderately useful”. Several (n = 8) noted that the young man’s disability was distracting and that they would have preferred to see someone without challenges in the film. The majority (n=14) stated that the film is too long. Most significant to this project: 7 youth with high-functioning ASD withdrew their consent to participate in the imaging appointment after watching the video, suggesting that the information provided exacerbated their anticipatory anxiety instead of diminishing it. Next Steps: A shorter, clearer demonstration of the imaging appointment is needed. Youth with high-functioning ASD and anxiety likely require a different approach to preparing for an imaging visit and may do better visiting and completing a very brief practice trial in the lab instead of providing the film/social story in advance.

Task 6. Interim Analyses. (a) Interim statistical analyses of data obtained from imaging and behavioral/cognitive assessments. This will be done annually in preparation for

progress reports and IRB renewals. (b) Annual reports and continuing review IRB proposals will be written. Progress: Done. Due to low rates of image visit completion, data analysis efforts were primarily directed toward behavioral data.

Task 7. Final Analyses and Report Writing. (a) Final analyses of data from behavioral and imaging experiments will be performed. (b) A final report and initial manuscripts will be prepared for submission to peer-reviewed journals. Progress: Done with behavioral data (See Tables 1 -3 in Appendix A). Partially met with imaging data.

MEG Data Collection: MEG data were collected for fewer participants than anticipated, due to unanticipated scheduling difficulties with potential participants. MEG imaging was successfully completed by 5 participants. Although this was short of the study goal, much was accomplished through the imaging efforts in this study. First, as described, the development and testing of the MEG video used in the current study showed this to be a successful strategy for reducing anxiety for participants with ASD during MEG scanning procedures. As such, this video has since been used in other studies at the MEG laboratory in which children with ASD or other developmental disorders are recruited. Additionally, the development of the novel motion correction technique for this study, described above, represents a significant benefit to ongoing MEG scanning efforts. Furthermore, the picture matching task, one of the main tasks in the current study, was developed and tested as part of this study. Although fewer participants completed the task than was hoped, the development of this task, which aims to identify mismatch deficits without requiring a verbal response, will benefit future studies of neuronal biomarkers of ASD. As such, the development and testing of this task represents a considerable and useful accomplishment of the current study. Figures 2 and 3 show MEG data during the picture matching task for a representative study participant (participant with ASD who is nonverbal). Figure 2 demonstrates the average MEG response across the task (showing the mismatch negativity response) for all channels. Figure 3 shows the response when averaged across all channels.

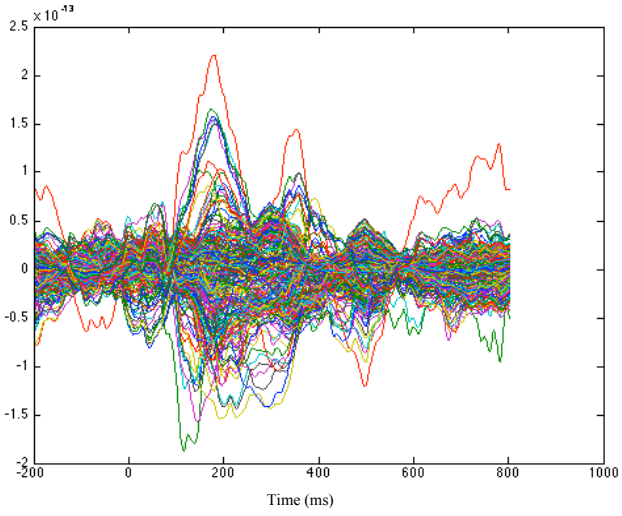


Figure 2. Average MEG signal (all channels) across picture matching task.

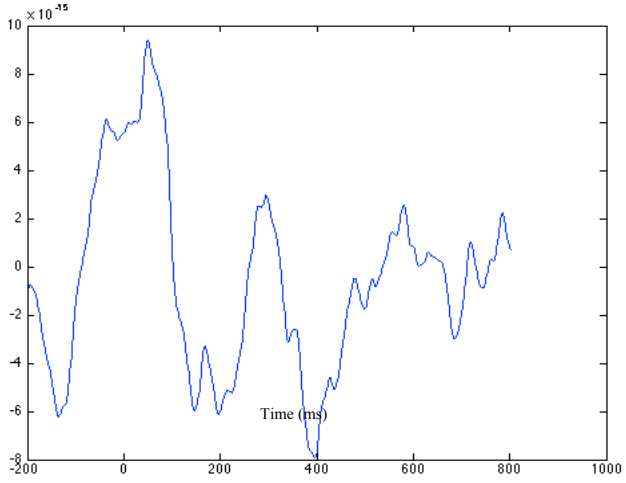


Figure 3. Average MEG signal (average of all channels) across picture matching task.

Opportunities for Professional Development and Training. Through this project, 2 advanced graduate students in clinical psychology and 1 postdoctoral fellow in psychology completed training in the administration and scoring of diagnostic measures for autism (ADOS & ADI). One graduate student also completed a course on using MATLAB to construct experiments for use in the imager. As part of the recruitment efforts for this study, the PI (Dr. Hepburn) conducted 9 community workshops for families of youth with ASD (described previously under Task 3). The postdoctoral fellow (Cardon) and the original PI of this project (McFadden-Legget – then a post-doc, now an Asst Professor at UC-Denver) both completed a 3-credit course in Autism Spectrum Disorders across the Lifespan, taught by Dr. Hepburn through the LEND program. Drs. Legget and Cardon are also active members of the Developmental Psychobiology Research Group and presented their work to their peers 2 times per year across all 3 years of this study.

Dissemination of Results. We presented the film, social story and procedures for engaging youth with ASD in imaging studies at a regional conference hosted by the Developmental Psychobiology Research Group in 2013 and 2015. We also sent participating families a brief summary of the results of our work comparing the film with the social story. Dr. Hepburn participated in a Special Interest Group on Minimally Verbal Youth at the International Meeting of Autism Research (IMFAR) in 2013, 2014 and 2015 and helped to draft the SIGs recommendations concerning strategies for improving research engagement.

Plans for Next Reporting Period. This is the final report; nothing to report.

4. Impact:

There are 3 innovations that have emerged from this study that have the potential to improve the engagement of minimally verbal youth with ASD in neuroimaging research. First, the two passive auditory tasks that were developed, piloted, revised and finalized during this study are available for other investigators interested in measuring auditory processing via passive tasks. (See Appendix C; McFadden et al., 2013).

Second, lessons learned in preparing youth with ASD for imaging protocols suggest that different approaches are necessary for different subgroups. Less verbal youth responded better to repeated readings of a simple, pictorial social story. (See Appendix B). More verbal youth preferred a film to a social story, but may respond better to a shorter film that focuses on a typically-developing/high-functioning youth. The film also needs to be edited to reduce the focus on the negative/challenging aspects of the experience and instead provide a more encouraging, positive glimpse at the imaging experiments. Brief practices in the machine may also help to promote engagement.

Third, the motion correction algorithms worked well for participants who were able to attend an imaging appointment and were willing to stay in the machine for up to 3 minutes. Peter Teale, the electrical engineer for the Magnetoencephalography Laboratory, designed a new circuit board to use with the head coil interface during MEG data collection, with the goal of measuring head motion during MEG recordings for this study. This device was used during data collection to allow for movement correction during data analyses.

A magnetic dipole phantom was used to test the efficacy of applying our newly developed motion correction technique to MEG data in which the subject moves repeatedly during data recording. During recording, the phantom was moved, such that there were 5 shifts in position throughout the MEG recording. The technique we have developed (with MEG lab electrical engineer Peter Teale and MEG lab physicist Eugene Kronberg; see circuit design in Appendix) involves the use of high-frequency signals outside a range that would be observed from measured brain activity. By localizing these signals throughout the recording, we are then able to correct for movement occurring during recording. In Figure 1, below, the data were filtered to remove these high-frequency signals (after using them for localization of movement). Data were then corrected for movement using the calculations derived from the high-frequency signals. The average MEG waveform is shown before motion correction (panel A) and after motion correction (panel B). The scale of the signal is the same in both panels A and B. Noise in the recording created by subject movement can result in a cancellation of signal. The larger amplitude shown in Panel B demonstrates that we experience less signal loss when using motion correction than we would if we did not incorporate motion correction. As such, given that the subjects in this project are likely to move during MEG recording, the use of our motion correction technique will result in higher quality data than would be possible without this technique. Furthermore, goodness of fit and correlation, as measured by use of the phantom, were increased when applying motion correction compared to when we did not apply the correction.

Panel A (before correction) **Panel B (after correction)**

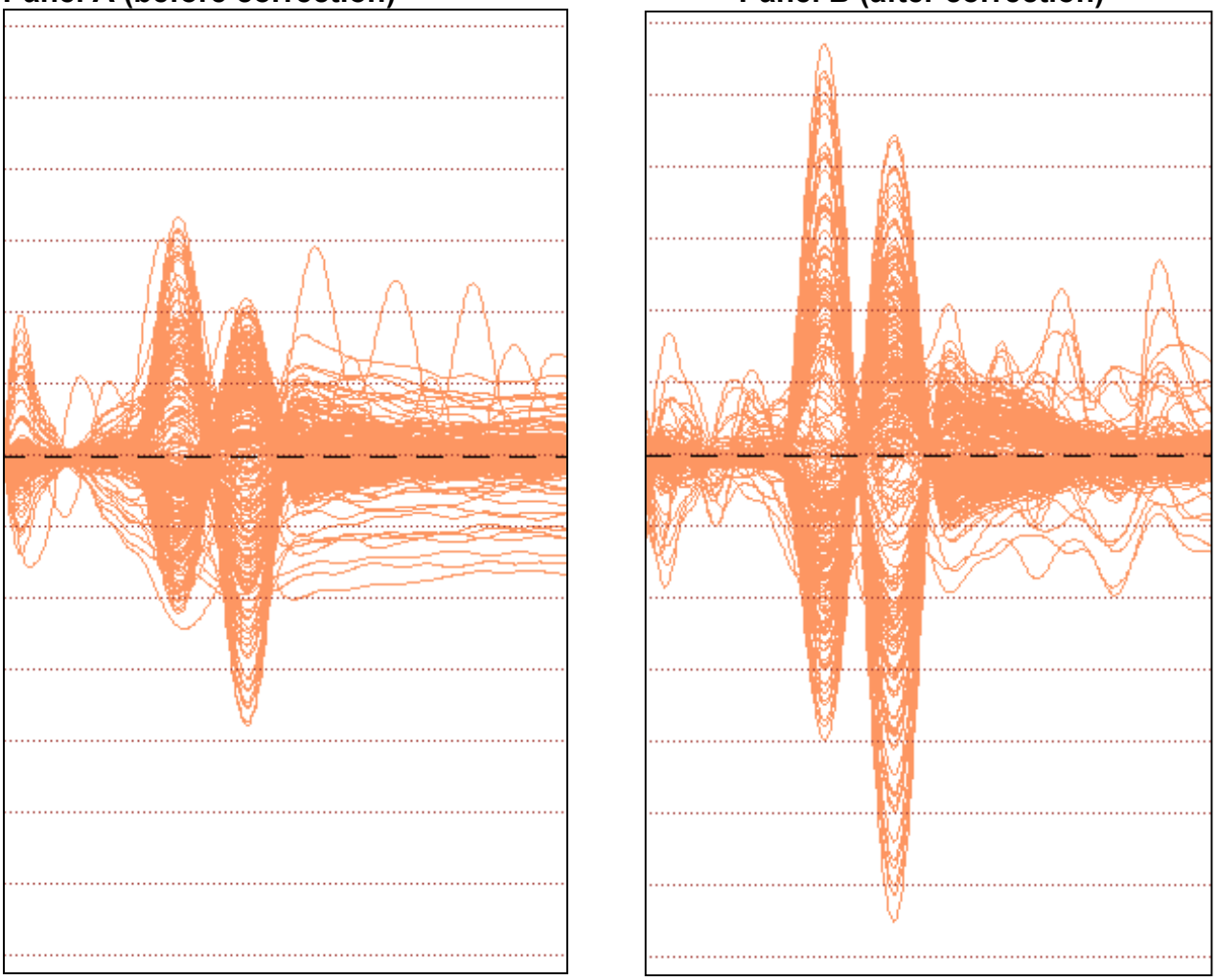


Figure 1. Demonstration of decreased signal loss due to subject movement when using movement correction (Panel B) compared to not using movement correction (Panel A).

5. Changes/Problems:

(Changes in Approach/Reasons for Changes/Anticipated Problems & Plans)

a. Staff/Leadership Changes. This project was initiated by a Kristina McFadden Legget, PhD, then a postdoctoral fellow working under the supervision of Don Rojas, PhD and Susan Hepburn, PhD. Dr. Rojas oversaw several neuroimaging studies of ASD at the University of Colorado until he took a faculty position at Colorado State University in 2014. Dr. Hepburn, a clinical psychologist and Director of Research for the UCEDD and LEND programs at the University of Colorado provided clinical training and oversaw the research qualification and phenotyping for the participants in Dr. Rojas's studies. Dr. Legget wrote the grant for this project and was PI for Year 1, with Drs. Rojas and Hepburn as mentors. During Year 2, Dr. Legget obtained a K award from NIH, requiring her to cease all other funded research projects. Given that Dr. Rojas had relocated to CSU, Dr. Hepburn agreed to serve as PI for the second and final year of the project. Dr. Legget assisted some, but was actively engaged in her K-award; thus

we needed to build a new research team to finish this project. We recruited Isabelle Buard, PhD; an instructor who took over the imaging component; and hired two PRAs from the Clinical Psychology doctoral program at the University of Denver, and engaged a new postdoctoral fellow (Dr. Garrett Cardon) in the imaging projects. These staff/PI changes were approved by UC-Denver and by the Department of Defense; however, the time required to complete the change administratively and to update all human subjects approvals to include the new team and the revised desensitization procedures took up several months of year 2. Thus, we requested a no-cost extension and tried to meet our goals through one more year of effort. Overall, the staff and leadership changes required additional time, but the team was able to coordinate project tasks efficiently – particularly through the behavioral battery.

It is important to acknowledge that Dr. Hepburn also left UC-Denver in the spring of 2016 for a professorship at CSU. Thus, correspondence following the submission of the Year 3 final report did not reach her until colleagues at UC-Denver alerted her to the need to revise the final report. We regret this, and now recognize that we should have initiated a clearer communication about the PIs change in jobs, even though the change occurred simultaneously to the end of the project period.

b. Study Workflow. The impact of this project would have been improved if we had figured out a more efficient flow of participants from the behavioral/ diagnostic/qualifying visits to the imaging appointments. Although offering to provide an updated clinical report that summarized the results of the standardized diagnostic/developmental evaluations improved our participant recruitment; we were disappointed to see so many families stop participating in the study once their behavioral portion was completed, thus opting out or not scheduling the imaging appointment, even with multiple attempts to engage them in that portion of the study. In the future, it may be more effective to provide the report and the incentives after completion of the imaging visit.

c. Participation Ascertainment. Recruitment for this study was challenging, as many youth were hesitant about participating in the MEG component. The community workshops worked well for bringing more families of youth with ASD into the participant recruitment flow; however, our efforts to recruit healthy controls were insufficient to meet our enrollment goals. Future studies that include healthy controls will require a very specific, proactive plan for engagement; possibly by offering more incentives or different kinds of incentives (i.e., class credit, volunteer certificate).

Changes that Had a Significant Impact on Expenditures – None; other than requesting permission for a no-cost extension so that we could have more time to realize our recruitment and data collection goals.

Changes in human subjects protections – None. We encountered no adverse events or human subjects concerns across the study period. We changed the wording of our consent forms to make them more “participant friendly” in Year 2 and those changes were approved by the IRB and HRPO.

Vertebrate animals: N/A
Biohazards: N/A

6. Products:

a. Publications, Conference Papers & Presentations:

2013

McFadden KL, Hepburn S, Schmidt GL, Winterrowd E, Rojas DC (2013). Abnormalities in gammaband responses to language stimuli in first-degree relatives of children with autism spectrum disorder. BMC Psychiatry, 12: 213. PMCID: PMC3557147

McFadden KL, Steinmetz SE, Hepburn S, Tregellas, JR, Rojas, DC (2013). Steady-state gamma-band responses in children with autism spectrum disorders during an auditory oddball task. Presented at the American College of Neuropsychopharmacology (ACNP) 52nd Annual Meeting, Hollywood, FL.

McFadden, K., Steinmetz, S., Hepburn, S., & Rojas, D. (2013). Steady-state Gamma-band Responses in Children with Autism Spectrum Disorders During an Auditory Oddball Task. *Neuropsychology,* 38 (2), S459-S459.

2014

McFadden KL, Rojas DC (2013). Electrophysiology of Autism. In M. Fitzgerald (Ed.), Autism (Book 2). InTechOpen. ISBN 980-953-307-552-0. DOI: 10.5772/53770.

McFadden KL, Steinmetz SE, Carroll AM, Simon ST, Wallace A, et al. (2014) Test-Retest Reliability of the 40 Hz EEG Auditory Steady-State Response. PLOS ONE 9(1): e85748. https://doi.org/10.1371/journal.pone.0085748

2016

Cardon, G., Hepburn, S., & Rojas, D. (2017). Structural covariance of sensory networks, the cerebellum, and amygdala in autism spectrum disorder. *Frontiers in Neurology, 8,* Article 615. doi: 10.3389/fneur.2017.00615.

Technologies or techniques

-MEG motion correction analysis pipeline (described in *Impact* section)
-Picture matching MEG task (described in *Impact* section)
- MEG motion correction equipment (see *Impact* section)
- MEG film for potential participants
-MEG Social Story (see Appendix B)

7. Participants and Other Collaborators:

The following personnel committed more than 1.0 months during Year 1 of this project:

Kristina McFadden, Ph.D.	Role = PI	1.80 calendar months
Susan Hepburn, Ph.D.	Role = Mentor/Co-PI	.24 calendar months
Don Rojas, Ph.D.	Role = Mentor/Co-PI	.24 calendar months
Erika Shelton, BS	Role = PRA	4.80 calendar months

The following personnel committed more than 1.0 months during Years 2 & 3 of this project:

Susan Hepburn, Ph.D.	Role = PI	1.44 calendar months
Isabelle Buard, Ph.D.	Role = Co-I, Technician	1.20 calendar months
Lisa Ankeny, M.S/	Graduate Assistant	2.40 calendar months

Caren Rhodes, M.Ed. Graduate Assistant 2.40 calendar months

In-kind consultation was provided by Donald Rojas, Ph.D., a colleague and collaborator of Dr. Hepburn's and Dr. McFadden's (original PI) in years 2 and 3. Dr. Rojas meets with Dr. Hepburn regularly to review the neuroimaging aspects of the study. Dr. McFadden continues to participate in scientific discussions concerning the project. Dr. Peter Teale and Dr. Eugene Kronberg also provided technical assistance in-kind on the motion detection aspect of the project. Dr. Garrett Cardon (postdoctoral fellow) also participated on the project in years 2 and 3 as an in-kind contribution and to receive his training in the diagnostic measures.

Two non-profit educational/day programs serving persons with ASD in the greater Denver community (Joshua School, Temple Grandin School) have collaborated with the research team to generate awareness of the study and to reach families of minimally verbal youth. Members of the Parent/Family Faculty of the Leadership Education in Neuro-developmental Disorders (LEND) Program at JFK Partners (University Center for Excellence in Developmental Disabilities; Kristen Kaiser, Jill Pidcock) have provided feedback on the participant orientation kit and have consulted with the team on the wording of consent forms and flyers.

8. Special Reporting Requirements: n/a

9. Appendices:

A. Tables 1-3: Participant Characteristics

B. Social Story

C. Publications/Conference Abstracts

Appendices

Appendix A Tables 1 -3 Participant Characteristics

Table 1 Participant Characteristics: Total Sample (n=49)

Sex % Male	73.50
Age (months) Mean (SD) Range	158.20 (50.30) 61 - 251
Age (years) Mean (SD) Range	13.18 (4.19) 5 – 21 years
Race n (%) African-American Caucasian Asian Native American	7 (14.4%) 40 (81.6%) 1 (2%) 1 (2%)
Ethnicity n (%) Hispanic	11 (22.4%)
Nonverbal IQ Estimate[1] Mean (SD) Range	69 (18.30) 45 – 110
Full IQ Estimate[2] Mean (SD) Range	96.09 (12.32) 76 -122
Token Test Standard Score[3] Mean (SD) Range	78.08 (30.94) 25 - 130

[1] n = 14
[2] n = 23
[3] n = 24

Table 2 Characteristics of Eligible Participants by Study Group (n = 39)

	Youth w/ ASD-Minimally Verbal (n = 14)	Youth w/ ASD-Verbal (n = 21)	Controls (Not ASD or DD) (n = 4)
Sex % Male	57.10%	85.7%	50%
Age (months) Mean (SD)	149.71 (58.86)	163.38 (47.91)	179.50 (21.55)
Range	62 - 223	61 - 251	149 - 197
Age (years) Mean (SD)	12.47 (4.90)	13.61 (3.99)	14.96 (1.79)
Range	5 – 19 years	5 – 21 years	12 – 17 years
Race n (%) African-American	2 (14.30%)	1 (4.8%)	1 (25%)
Caucasian	12 (85.78%)	19 (90.5%)	3 (75%)
Asian	--	1 (4.8%)	--
Native American	--	--	--
Ethnicity n (%) Hispanic	2 (14.30%)	4 (19%)	2 (50%)
Nonverbal IQ Estimate[4] Mean (SD)	66.09 (17.16)	--	
Range	45 – 98		
Full IQ Estimate[5] Mean (SD)	--	95.35 (14.02)	100.25 (6.95)
Range	--	76 - 122	90 - 105
Token Test Standard Score[6] Mean (SD)	41.71 (17.98)	94.31 (6.62)	102.67 (26.10)
Range	25 - 68	76 - 128	78 - 130

[4] n = 14
[5] n = 23
[6] n = 24

Table 3 Characteristics of Participants Not Eligible for Study (n = 10)

Sex % Male	80%
Age (months) Mean (SD) Range	145.78(53.66) 68 - 211
Age (years) Mean (SD) Range	12.15 (4.47) 5 – 18 years
Race n (%) African-American Caucasian Asian Native American	3 (30%) 6 (60%) -- 1 (2%)
Ethnicity n (%) Hispanic	3 (30%)
Nonverbal IQ Estimate[7] Mean (SD) Range	75.67 (12.89) 65 – 90
Full IQ Estimate[8] Mean (SD) Range	100.00 (11.32) 92 -108
Token Test Standard Score[9] Mean (SD) Range	48 (0) --

[7] n = 3
[8] n = 7
[9] n = 1

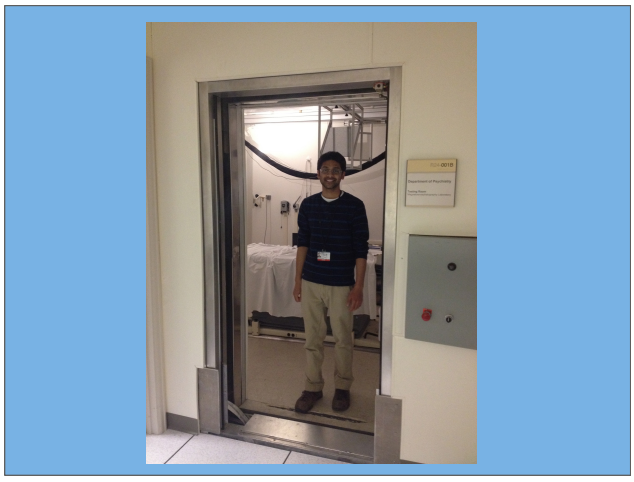
APPENDIX B

MEG Picture Story (Note: We present this story to the participants as a scrollable pdf with voicover (optional) on a portable USB. They receive this story and information sheets and a short film about the MEG appointment).



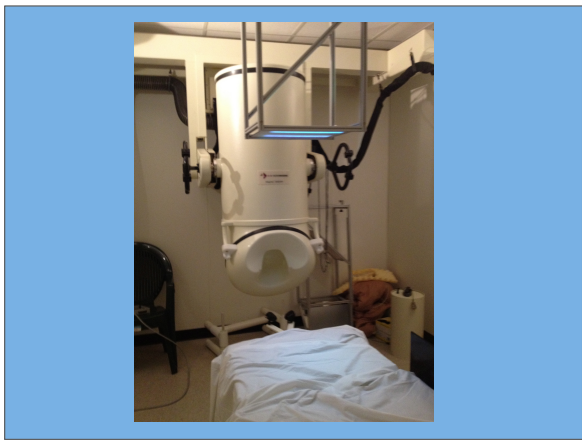
David is going to meet with a scientist who studies the human brain.

The scientist uses a machine called an "MEG" to measure brain activity.



This is the room where the MEG machine is. The machine is very powerful. Just like an x-ray machine, its okay to be near the machine when its working sometimes, but not all the time. That's why the room has large doors that shut tightly.

If David decides to do the study, he will only be in the room for a short time – about as long as an episode of his favorite show – The Big Bang Theory.



This is what the machine looks like inside the room. A person lays down on the table and the scientist gently lowers the machine so that it is sitting above the person's head. The person's body is outside of the machine.



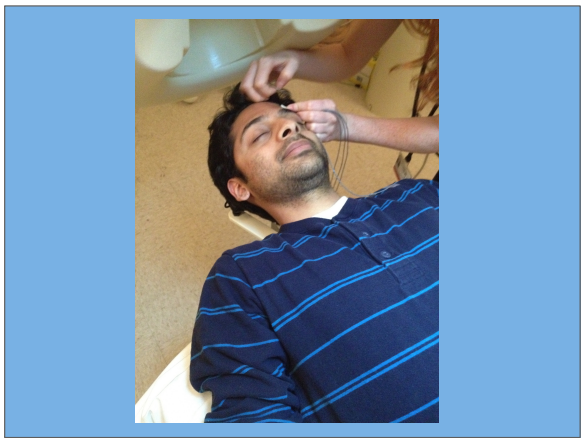
David sits on the table and looks at the machine. It's smooth, cold and clean. Right now, it's quiet, but when the scientist turns it on, it will make a humming and knocking sound. The sounds are not loud, but they keep going for several minutes at a time. It sounds like air being pumped into a tire.



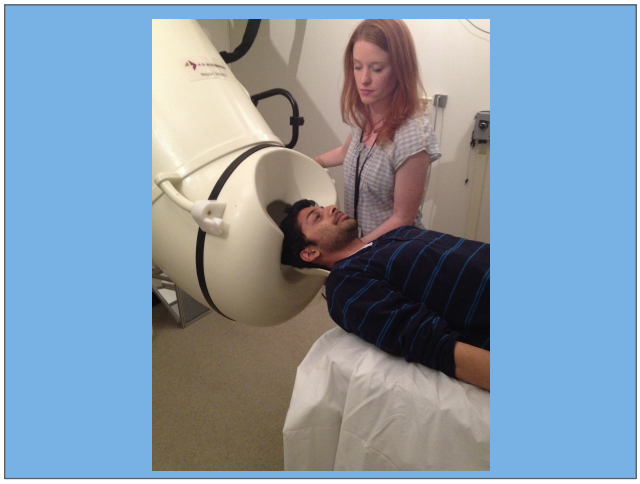
David lays down. He looks up and can see a computer screen showing clips from the movie “Avatar”. The scientist gave him a choice of 3 different movies. He liked “Avatar” best.



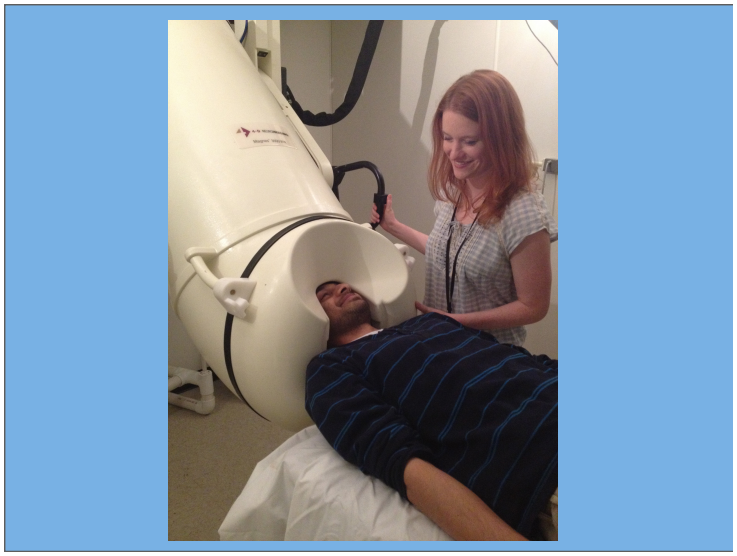
The scientist rolls David’s table under the MEG machine. He is still watching “Avatar”. The scientist is getting the machine’s sensors ready – these are small sticky pieces of plastic that will be placed on David’s face and head. Then, they will connect to the MEG machine. Sensors do not hurt. They feel like putting on a bandaid.



The scientist gently puts the sensors on David's head. This takes a few seconds for each sensor. There are about 10 sensors.

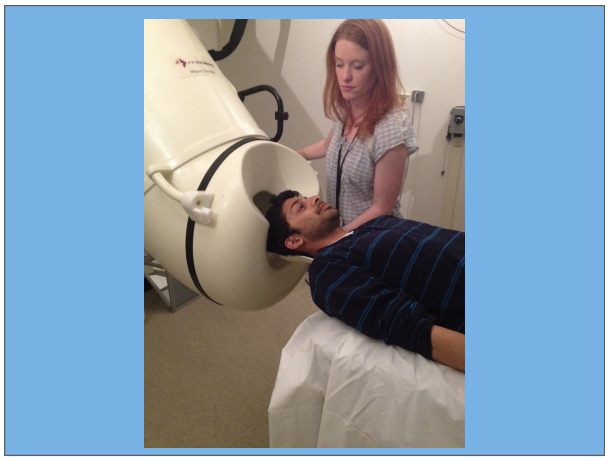


The scientist gently brings the machine closer to David. She guides his head so that it is resting comfortably. David stays still and the scientist moves the machine so that it is at the correct angle. Everything is quiet – except for the Avatar movie.



This is what it looks like when the machine is in the correct position. It works like a helmet. To David, it just feels like he is wearing a big hat that gently touches his face and goes all the way to the ceiling. It is still quiet.

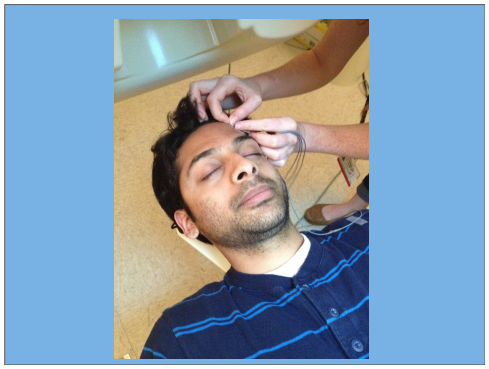
The scientist asks David if he is comfortable. Then, she asks him to stay still for about 5 minutes. She's going to leave the room and turn on some sounds. She wants him to listen and try not to move. He doesn't have to do anything else.



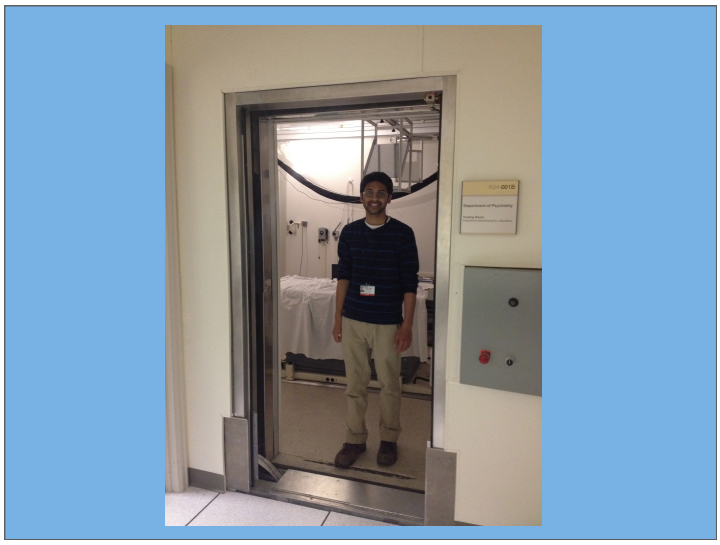
Five minutes later, the scientist comes back and moves the machine back and away from David's head.

David makes a joke that he took a little nap.

The scientist thanks him for being so still and resting like he did.



The scientist gently takes the sensors off of David's head. It doesn't hurt at all.



David is all done with the MEG study!

The scientist thanks him for his time and gives him a Gift card to spend later.

David has helped the scientist and is ready to go home.

Thanks David!

Appendix C: Selected Publications

OPEN ACCESS Freely available online

PLOS ONE

Test-Retest Reliability of the 40 Hz EEG Auditory Steady-State Response

Kristina L. McFadden[1,2], Sarah E. Steinmetz[1,2], Adam M. Carroll[1], Steven T. Simon[2], Alissa Wallace[1,2], Donald C. Rojas[1,2]*

1 Department of Psychiatry, University of Colorado Anschutz Medical Campus, Aurora, Colorado, United States of America, **2** School of Medicine, University of Colorado Anschutz Medical Campus, Aurora, Colorado, United States of America

Abstract

Auditory evoked steady-state responses are increasingly being used as a marker of brain function and dysfunction in various neuropsychiatric disorders, but research investigating the test-retest reliability of this response is lacking. The purpose of this study was to assess the consistency of the auditory steady-state response (ASSR) across sessions. Furthermore, the current study aimed to investigate how the reliability of the ASSR is impacted by stimulus parameters and analysis method employed. The consistency of this response across two sessions spaced approximately 1 week apart was measured in nineteen healthy adults using electroencephalography (EEG). The ASSR was entrained by both 40 Hz amplitude-modulated white noise and click train stimuli. Correlations between sessions were assessed with two separate analytical techniques: a) channel-level analysis across the whole-head array and b) signal-space projection from auditory dipoles. Overall, the ASSR was significantly correlated between sessions 1 and 2 ($p<0.05$, multiple comparison corrected), suggesting adequate test-retest reliability of this response. The current study also suggests that measures of inter-trial phase coherence may be more reliable between sessions than measures of evoked power. Results were similar between the two analysis methods, but reliability varied depending on the presented stimulus, with click train stimuli producing more consistent responses than white noise stimuli.

Citation: McFadden KL, Steinmetz SE, Carroll AM, Simon ST, Wallace A, et al. (2014) Test-Retest Reliability of the 40 Hz EEG Auditory Steady-State Response. PLoS ONE 9(1): e85748. doi:10.1371/journal.pone.0085748

Editor: Natasha M. Maurits, University Medical Center Groningen UMCG, Netherlands

Received July 5, 2013; **Accepted** December 2, 2013; **Published** January 22, 2014

Copyright: © 2014 McFadden et al. This is an open-access article distributed under the terms of the Creative Commons Attribution License, which permits unrestricted use, distribution, and reproduction in any medium, provided the original author and source are credited.

Funding: Funding for this study was provided by NIH grants R01 MH08280, R01 MH081920 and a NARSAD Independent Investigator Award to DCR, and NIH/NIMH training grant T32 MH015442 for KLM. The funders had no role in study design, data collection and analysis, decision to publish, or preparation of the manuscript.

Competing Interests: The authors have declared that no competing interests exist.

* E-mail: Don.Rojas@ucdenver.edu

Introduction

Oscillatory activity in the brain is thought to be an important component of brain function and integration [1,2]. Neuronal oscillations in the gamma range (~30–80 Hz) have been implicated in a number of processes, including attention [3–5], working memory [6,7], early sensory processing [8,9], perceptual binding [10,11], and language [12–15]. Temporal integration of auditory information in the brain can be studied using the auditory steady-state response (ASSR), which was initially investigated by driving the response using clicks presented at 40 Hz [16,17]. Although steady-state responses are being used increasingly as a marker of brain function, particularly in psychiatric disorders [18–21], no studies have investigated the test-retest reliability of this response. Determining the reliability of the ASSR will be essential for the continued use of this response in studies comparing patient and control populations.

Previous studies have found abnormalities in the ASSR in such disorders as autism [20], schizophrenia [18,21–26], and bipolar disorder [19,27,28]. Similar abnormalities have also been found in first-degree relatives of patients with these disorders [29–31]. The ASSR can be elicited by a variety of stimuli, including clicks presented at high rates or by tone or white noise stimuli amplitude-modulated at the same rates, where 40 Hz driving appears to produce the largest ASSR in adult studies [16,20,31–38]. Gamma-aminobutyric acid (GABA) is thought to play an important role in the generation of the ASSR [39,40]. This relationship suggests that ASSR activity may serve as a marker of the efficiency of inhibitory mechanisms in the brain, although most of what is known of this potential is from studies of spontaneous gamma-band responses, not from steady-state responses driven in the gamma-band range [41–43]. GABA mechanisms are also thought to be dysfunctional in autism [44–46], schizophrenia [39,47], and bipolar disorder [48,49]. As such, the ASSR may be an important potential endophenotype (that is, an unseen, heritable phenotype) in these patient populations, and could prove highly useful for assessment during therapeutic development. In addition, this could advance knowledge of the underlying neurophysiology behind these disorders and further genetic and animal studies. Knowledge regarding the test-retest reliability of the ASSR will be important to establish its potential for use as a predictor variable or marker of outcome in clinical trials.

Test-retest reliability has been well documented for various EEG-measured event-related potentials (ERPs) [50–54] and for neuronal activity in low frequency bands [55–58]. However, relatively few studies have focused on the reliability of auditory responses in the gamma range. While evoked gamma-band activity has demonstrated between-session consistency in response to visual stimuli [43,59–61], little is known regarding reliability in

the auditory domain. A preliminary investigation of 6 individuals found amplitude of the peak auditory evoked *transient* gamma-band response to be strongly correlated between sessions in response to white noise stimuli [62]. However, the reliability of the auditory *steady-state* response has not yet been systematically studied. This is an important gap in the literature, since many of the auditory phase-locked gamma-band findings in autism and schizophrenia have emerged from steady-state stimulation approaches.

The purpose of the current study was to investigate between-session reliability of the ASSR as measured by EEG. Based on previous findings, we hypothesized that the ASSR would be significantly correlated between sessions spaced one week apart. While a future study including multiple time points will be important, an initial investigation of the response across one week seemed a reasonable starting point. Further, this time period was chosen with the intent of identifying reliability of the response for an interval of time commonly used in pharmacological trials. Establishing the reliability of this response spaced one week apart without pharmacological intervention will provide important information for future clinical studies utilizing this time period. Previous studies have found the type of stimulus to influence the strength of the ASSR [37,38,62]. Stimulus type has also been shown to influence reliability of *transient* responses in the gamma range [62]. As such, the current study assessed differences between the ASSR elicited by both amplitude-modulated white noise and click train stimuli, both of which have previously been found to elicit the ASSR [17,20,31,36,38]. Furthermore, to evaluate the impact of different analytical techniques on measures of ASSR reliability, two separate analytical methods were compared, one based on sensor-space analyses and the other on source reconstruction. We predicted, based on prior EEG studies of ERP reliability [63], that source reconstruction would improve the signal-to-noise ratio of the measures and result in higher test-retest reliability.

Methods

Participants

Nineteen participants (10 male, 9 female, mean age = 30.1+/− 8.8 years, range: 20.3–54.9 years) completed the study. Of these participants, 10.5% identified themselves as African American/Black, 5.3% as Asian, and 84.2% as Caucasian. Ethnic identities were separately ascertained; 21.1% of the sample was Hispanic and the remainder was non-Hispanic. Eligibility criteria required participants to have no personal history of a current or past neurological or Axis I psychiatric disorder, assessed by the SCID Screen Patient Questionnaire-Extended [64]. Participants were recruited via fliers and mass email postings.

Ethics statement

The human subjects protocol was approved by the Colorado Multiple Institutional Review Board. Written, informed consent was obtained from all participants, consistent with the guidelines of the Declaration of Helsinki.

Stimuli and paradigm

Participants completed two recording sessions separated by approximately one week (mean = 10.2, SD = 6.1 days apart, minimum of 5 days between sessions), and completed the same tasks in both sessions. Both were passive listening tasks, in which 200 trials of either white noise or click train stimuli were presented binaurally through foam insert earphones (Neuroscan, Inc., North Carolina, USA) at 75 dB SPL for 500 ms each, with an inter-trial interval of 1000 ms. All participants completed both the white noise and click noise stimuli tasks. White noise stimuli were 500 ms, 40-Hz amplitude-modulated (100 percent depth) white noise. Click stimuli were 40-Hz click trains in which each click was 2 ms in duration delivered every 25 ms for a total of 500 ms. All participants reported having normal hearing. As participant states and attention can impact the ASSR [36,38,65,66], all participants were asked to sit upright and to remain awake with their eyes open during the tasks, with a break given between tasks to maintain alertness. In addition, alpha power was monitored to ensure that participants' alertness did not vary systematically by task or session. Each task condition (white noise and click stimuli) lasted 5 minutes.

EEG recordings

Continuous EEG data were acquired using a 64-channel electrode cap (EASYCAP GmbH, Herrsching, Germany) with standard 10-10-system electrode placement [67]. Electrodes were placed on the outer canthi of both eyes and on the supra-orbit of the right eye to assess horizontal and vertical eye movements; an additional electrode was placed in the middle of the forehead to serve as the ground. Impedances were below 10 kΩ at all sites. ERP recordings were amplified using Neuroscan SynAmps 2 amplifiers (Neuroscan, Inc., North Carolina, USA), with a passband of .1–200 Hz and digitized at 1000 Hz. Recordings were average-referenced offline. Raw epoch data from this study, along with scripts to read the data, can be downloaded from Figshare (http://dx.doi.org/10.6084/m9.figshare.829584).

Data preprocessing

Offline, EEG data were preprocessed using Brain Electrical Source Analysis (BESA) 5.3 software (BESA GmbH, Grafelfing, Germany). Data were average-referenced and epochs of 1000 ms were created starting 200 ms prior to stimulus onset and lasting for 800 ms post-stimulus onset. Data were baseline-corrected to the mean of the pre-stimulus period and eye blink artifacts were removed using BESA's spatial filtering routine, which is based on the spatial components method for correcting eye artifacts [68–70]. Following eye blink correction, threshold-based artifact rejection was used to remove any epochs with activity greater than 100 μV. Data were then visually inspected and epochs with any additional movement or eye blink artifacts were removed from further analyses. Out of the 200 recorded trials, in the white noise task an average of 180.7 (SD: 23.8) trials were accepted and used for further analyses for session 1, with 184.2 (SD: 17.9) accepted for session 2. For the click train task, an average of 187.1 (SD: 32.9) trials were accepted for session 1, with 178.6 (SD: 20.8) accepted for session 2.

Statistical analyses

Method 1: Sensor-space analysis. Following preprocessing, time-frequency transformation was performed by complex demodulation [71,72] in BESA, which involves multiplication of the time-domain signal with sines (real) and cosines (imaginary) at each frequency of interest, followed by a Gaussian-shaped finite impulse response (FIR) low-pass filter and calculation of the absolute value. The full width at half maximum was 7.08 Hz and 63 ms, which was the effective resolution of the time-frequency transformation in our study. Within BESA, the time and frequency space was sampled in 2.5 Hz and 20 ms bins for further analyses. Time-frequency representations for both evoked activity, normalized to the pre-stimulus baseline, and inter-trial phase coherence (ITPC) were both derived from BESA [72–75] and then imported into Matlab (2009b; MathWorks, Inc., Natick, MA) using FieldTrip routines [76]. ITPC is a measure of event-related phase

locking across trials (inter-trial consistency), sometimes referred to as phase-locking factor (PLF), which ranges from 0 (purely non-phase-locked) to 1 (strictly phase-locked) [77,78]. For both tasks (white noise and click train stimuli), correlation routines in Matlab (using the Statistical Toolbox function, corcoeff.m) were used to determine between-session reliability for evoked activity and ITPC. For each channel (i.e., each of the 63 data channels), each individual time-frequency bin for session 1 was compared to the corresponding time-frequency bin for session 2 across all participants (for both the evoked response and ITPC). This was performed separately for each channel, and a false discovery rate (FDR), as described in Benjamini and Hochberg [79], of $q = 0.05$ was used to correct for multiple comparisons across channels and time-frequency bins. The FDR approach controls for the proportion of false positive findings among findings identified as significant (i.e., a q of 0.05 means that no more than 5% of the findings will be false positives). Additionally, the mean correlation coefficients at 40 Hz for each stimulus type (white noise vs. click train) and hemisphere (left vs. right) for absolute power, evoked power, and ITPC, were directly compared for significance using the Fisher r-to-z transformation.

A dependent-samples Student's t-test was run using FieldTrip routines to compare the ASSR (evoked power and ITPC; collapsed across sessions) between the white noise task and the click train task across all channels, using FDR for multiple comparison correction. For visualization purposes, the channel observed to have the highest amplitude at 40 Hz in the 200–500 ms window was identified from the grand averaged response. To assess the signal-to-noise ratio (SNR) for each task (across sessions) at FCz, we first calculated the mean squared coherence (MSC) as the ratio between 40 Hz signal alone (pre-stimulus baseline from −200–0 ms subtracted from the post-stimulus window of 200–500 ms) to 40 Hz signal plus noise (post-stimulus window of 200–500 ms). SNR was then calculated from MSC, as $SNR = (MSC/[1\text{-}MSC])^{1/2}$ (see [80] for details). Differences in SNR between tasks and hemispheres were assessed using paired t-tests in SPSS version 22 (IBM Corp., Armonk, NY).

Method 2: Signal-space projection. Signal-space projection (also called source-space projection or lead field synthesis [81,82]) was performed in BESA [73–75]. First, a grand average evoked waveform was computed across all participants, using averaged files created from the same preprocessed files used in the whole-head array method. A grand average was created across both tasks (white noise and click stimuli) and both sessions (1 and 2), so that source analysis differences between task and session could not influence the results. Having separate models for each could reduce reliability due to spatial variance between tasks and sessions. As such, there was a single grand average across all participants that included both tasks and sessions. Source analysis was performed by fitting left and right hemisphere equivalent current dipoles to the 40 Hz ASSR in the band-pass filtered (30–50 Hz) grand-averaged response between 200–500 ms (see Figure 1). The left (Talairach coordinates: $x = -46.3$, $y = -18.9$, $z = -2.6$) and right ($x = 44.7$, $y = -13.4$, $z = 4.9$) dipoles were located in primary auditory cortex, and the dipole model residual variance was 8.8%.

This source solution was used to project the raw data for each participant (i.e., the original preprocessed data) into the source domain using a source montage in BESA [83], resulting in a virtual electrode for each participant for left and right hemispheres (i.e., 2 data channels). The projection was done separately for each session (1 and 2) for each task (white noise and click stimuli). Time-frequency transformation was then performed in BESA, for the left and right hemisphere virtual electrodes for each session and task.

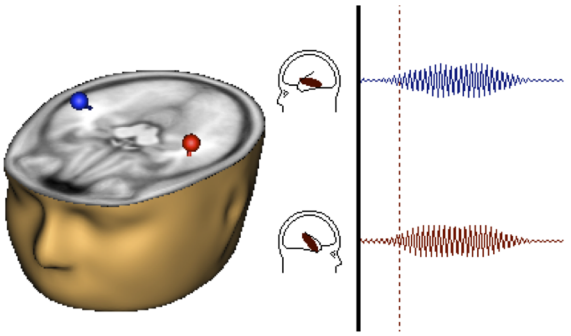


Figure 1. Signal-space projection. Representative diagram of placement of equivalent current dipoles and the resulting signal-space projected averaged waveform resulting from each dipole.
doi:10.1371/journal.pone.0085748.g001

The same time-frequency transformation parameters as in the sensor-level analysis were used (i.e., complex demodulation: −3 dB power full width at half maximum, resulting in effective time-frequency transformation resolution of 7.08 Hz and 63 ms; time and frequency space within BESA sampled in 2.5 Hz and 20 ms bins). Time-frequency representations for evoked activity and ITPC were then exported to Matlab for between-session correlation analyses. Multiple comparison correction was performed using FDR of $q = 0.05$. Furthermore, the mean correlation coefficients for FCz at 40 Hz for each stimulus type (white noise vs. click train) for absolute power, evoked power, and ITPC, were directly compared for significance using the Fisher r-to-z transformation. These were also compared with correlation coefficients from the sensor-level analysis.

As with the sensor-level analysis, a dependent-samples t-test was run using FieldTrip routines to compare the ASSR (evoked power and ITPC; collapsed across sessions) between the white noise task and the click train task, using FDR for multiple comparison correction. As described above, SNR was calculated from the MSC for each hemisphere for each task, across sessions. Task differences in SNR were assessed using paired t-tests.

Fourier analysis. In addition to the time-frequency analyses, Fourier analyses of epochs of the sensor-level and source-level data were conducted. Two time periods were analyzed: 1) between −300 and 0 ms pre-stimulus and 2) between 200 and 500 ms post-stimulus. The pre-stimulus and post-stimulus periods were zero-padded by 1000 ms and Hanning tapered to reduce edge effects. A Fast Fourier Transform (FFT) was used for Fourier analyses. For reliability analyses, the power at 40 Hz in the pre-stimulus and post-stimulus regions, as well as the relative power (post/pre) were statistically analyzed using regression analyses in SPSS. For the sensor-level statistics, power at electrode FCz was used. For the source-level statistics, power was analyzed separately for left and right auditory dipoles. As with the time-frequency analyses, SNR was calculated from the MSC for each task, across sessions. Differences in SNR between tasks were assessed using paired t-tests.

Alpha power. Because of the passive nature of the tasks, we also quantified alpha power during the first and last minutes of each 5-minute session. Continuous data for those 60-second periods were segmented into consecutive 1-second Hanning-tapered epochs, upon which an FFT was calculated to derive the power of alpha (8–12 Hz). Only alpha power at electrode Oz was used for this analysis. Differences between the first and last 60 seconds of each session for each task were assessed using paired

samples t-tests in SPSS, as were task (white noise vs. click train) and session (session 1 vs. session 2) differences.

Results

Method 1: Sensor-space analysis

A plot of the grand-averaged response to click train stimuli for each individual channel can be seen in supporting information (Figure S1). Although the click stimuli appeared to evoke a greater ASSR (both evoked and ITPC) compared to the white noise stimuli, differences between the two tasks in either the evoked response or ITPC, assessed across all time-frequency voxels, were not significant after correcting for multiple comparisons. Means for the absolute 40 Hz response in both the pre-stimulus (−200–0 ms) and post-stimulus window at FCz are shown in Figure 2, for both the time-frequency and Fourier transformed data. These data demonstrate significantly increased 40 Hz power to the click train stimuli compared to white noise stimuli in the window of the steady-state response (200–500 ms) for the Fourier analysis (Session 1: $p = .017$, Session 2: $p = .013$). However, this difference was not significant in the time-frequency analysis. The signal-to-noise ratio (SNR) for the ASSR (40 Hz, 200–500 ms) was also calculated across sessions for FCz (see Table 1). Within each task, there were no significant differences in SNR between sessions 1 and 2, in either the time-frequency or Fourier analyses. However, SNR for the click train stimuli was significantly greater than that for the white noise task across both time-frequency and Fourier analyses at FCz.

The correlation results for the comparison between sessions 1 and 2 for FCz for each task are shown in Figure 3. Plots of significant ($p<0.05$; FDR-corrected for multiple comparisons) correlations between time-frequency bins in session 1 compared to session 2 for each individual channel can be seen in supporting information (Figure S2). Means and ranges of correlation coefficients for the ASSR (40 Hz, 200–500 ms) for FCz are detailed in Table 2 for each task (white noise stimuli and click stimuli) for each measure (evoked power and ITPC). For both tasks, ITPC appeared to be more reliable between sessions than the evoked response. However, comparisons of the mean correlation coefficients at 40 Hz did not find any significant differences between ITPC and evoked responses. Overall, responses to the click stimuli appeared to be more reliable between sessions than those to the white noise stimuli. This can be seen in the figure depicting FCz, in which reliability for both the evoked response and ITPC is more evident for the click stimuli compared to the white noise stimuli. Results from the Fourier analysis are shown in Table 3. As with the time-frequency data, responses to click train stimuli appeared more reliable across sessions at FCz than responses to white noise stimuli. Indeed, the correlation between sessions 1 and 2 was not significant for white noise stimuli, but was significant for click train stimuli. Furthermore, across the whole channel array, a greater number of channels showed statistically significant ($p<0.05$, FDR-corrected)

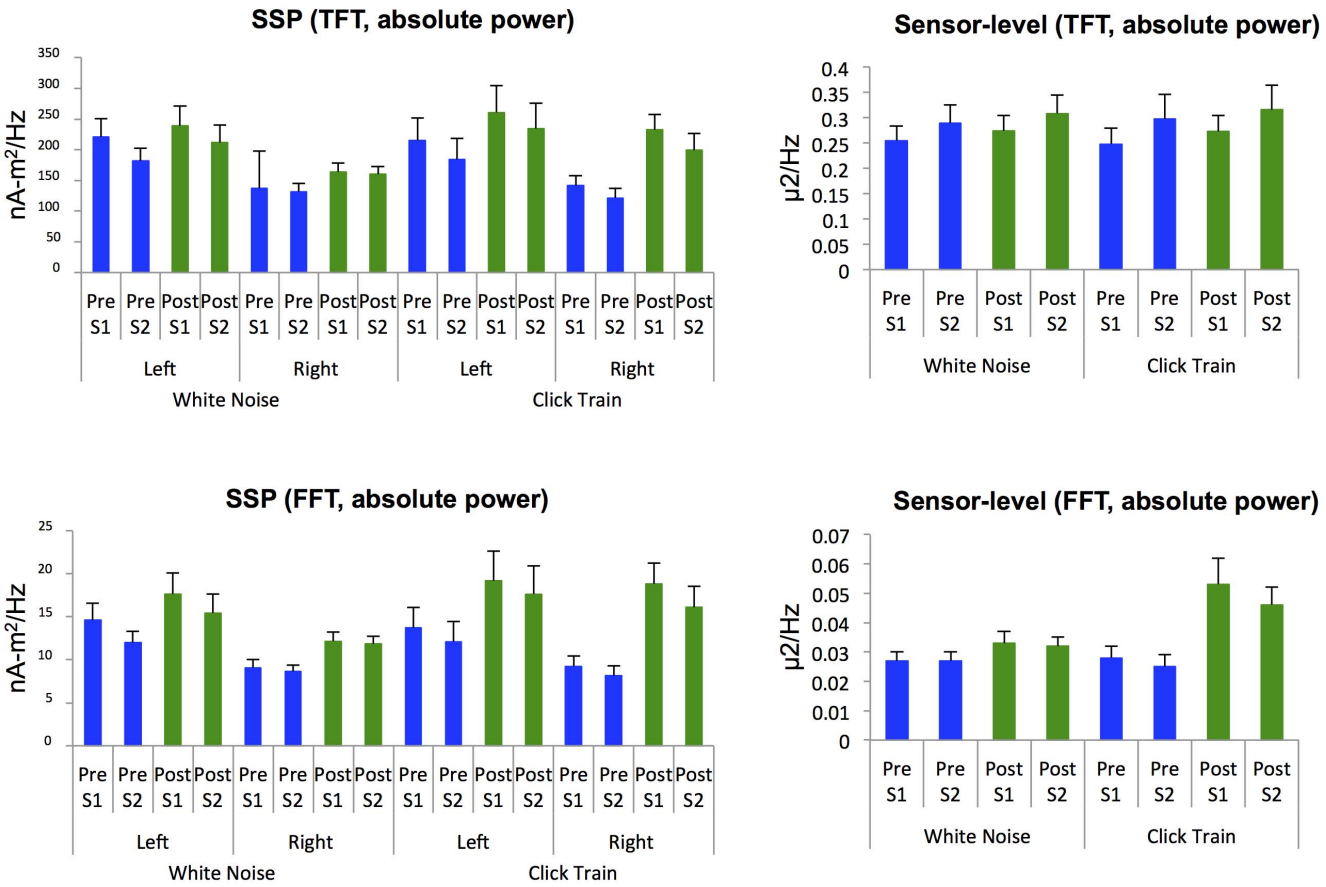


Figure 2. Average absolute power at 40 Hz. Absolute power for both the pre-stimulus window (Pre; −200–0 ms for TFT, −300–0 ms for FFT) and post-stimulus window (Post; 200–500 ms), for both session 1 (S1) and session 2 (S2) for both the white noise and click train stimuli. Results are shown for signal-space projected (SSP) and sensor-level (at FCz) data. TFT: time-frequency transformed data; FFT = Fast Fourier transformed data.
doi:10.1371/journal.pone.0085748.g002

Table 1. Signal to noise ratio (SNR) across sessions for the auditory steady-state response (40 Hz, 200–500 ms).

				Click Train		White Noise		CT vs. WN
	Method	**Channel**	**Measure**	**Mean**	**SD**	**Mean**	**SD**	**p**
TFT	Sensor	FCz	EP	.33	.12	.29	.10	*
		FCz	ITPC	2.52	.65	1.82	.56	***
	SSP	Left	EP	.44	.21	.30	.14	**
		Right	EP	.75	.34	.47	.18	**
		Left	ITPC	2.05	.68	1.49	.58	**
		Right	ITPC	2.45	.77	1.99	.54	*
FFT	Sensor	FCz	EP	.84	.39	.44	.14	***
	SSP	Left	EP	.60	.25	.42	.19	**
		Right	EP	.93	.43	.61	.22	**

CT = click train; WN = white noise; SD = standard deviation; TFT = time-frequency transformed data; FFT = Fast Fourier transformed data; ITPC = inter-trial phase coherence; SSP = signal-space projection; EP = evoked power (absolute). Significant left vs. right hemisphere comparisons: TFT SSP EP (click train***; white noise*); TFT SSP ITPC (click train*; white noise*); FFT SSP EP (click train**; white noise*).
*p<0.05;
**p<0.01;
***p<0.001.
doi:10.1371/journal.pone.0085748.t001

between-session correlations in the range of the ASSR (40 Hz, 200–500 ms) for the click train task (evoked: 29 channels; ITPC: 51 channels) compared to the white noise task (evoked: 7 channels; ITPC: 30 channels). However, when directly comparing the mean correlation coefficients at 40 Hz between click train and white noise stimuli, this comparison was only significant for the normalized evoked response (200–500 ms) at FCZ (see Table 2).

As would be anticipated for the click train stimuli, because there is stimulus energy at 40 Hz and its harmonics for this stimulus, a harmonic response at 80 Hz can be seen in both the grand-averaged data and correlations for the click train stimuli, particularly for ITPC. This is also seen, to a lesser extent, in response to the white noise stimuli, suggesting this response is a result of a harmonic to the 40 Hz activity in the brain rather than just to the 40 Hz stimuli, because there is not significant stimulus energy at 80 Hz in the white noise stimulus (above any other frequency). This is an expected effect, as previous studies have found that the brain response to a harmonic can be as strong as that to a stimulus, and may be localized at least partially independently of the fundamental stimulus response generator

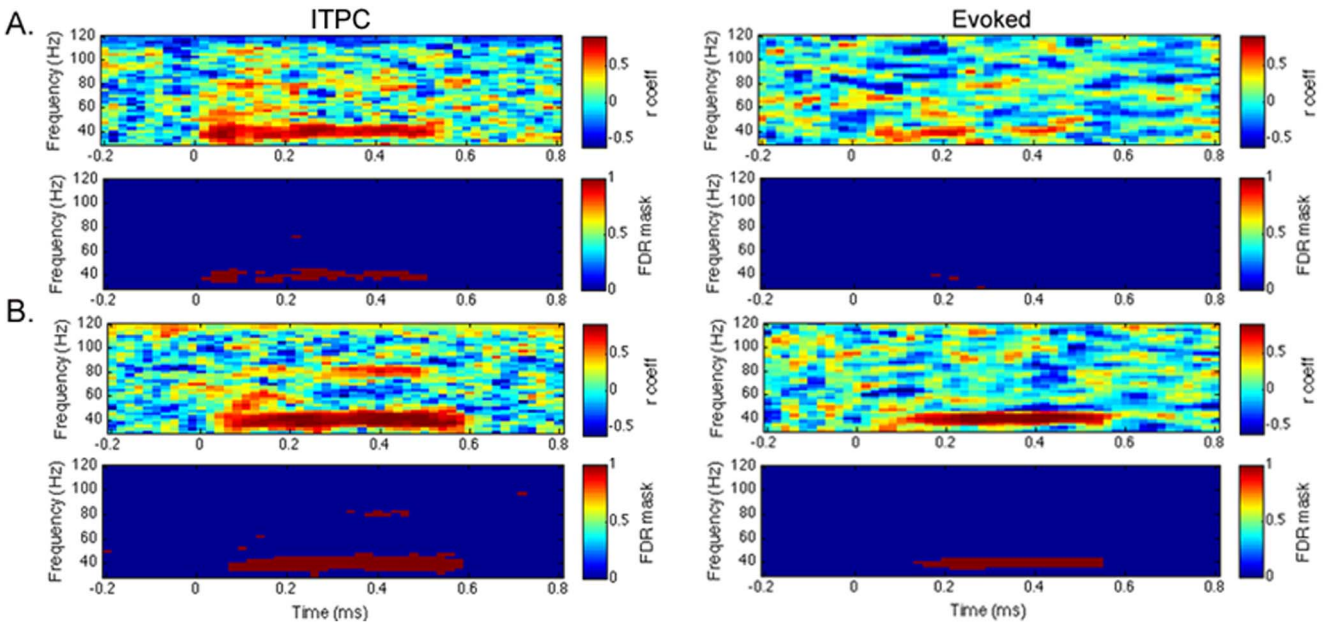


Figure 3. Example of correlation results. Correlation results between sessions 1 and 2 for inter-trial phase coherence (ITPC) and evoked activity for white noise stimuli (A) and click train stimuli (B) for the sensor-level analysis at the channel with the peak 40 Hz auditory steady-state response (FCz). In each plot, the first row shows the correlation coefficient (r coeff) and the second row shows correlations that were significant following multiple comparison correction (FDR, $q = 0.05$; 0/blue = not significant, 1/red = significant).
doi:10.1371/journal.pone.0085748.g003

Table 2. Correlation values (Pearson's r) between sessions 1 and 2 for the auditory steady-state response (40 Hz): time-frequency analyses.

				Click Train			White Noise			CT vs. WN
Method	**Chan**	**Measure**	**Time**	**r**	**SD**	**Range**	**r**	**SD**	**Range**	**p**
Sensor	FCz	Absolute EP	Pre	.42	.04	.38–.48	.62	.04	.55–.68	ns
	FCz	Absolute EP	Post	.44	.04	.38–.50	.58	.07	.45–.68	ns
	FCz	Normalized EP	Post	.90	.03	.83–.94	.50	.22	.14–.75	**
	FCz	ITPC	Post	.89	.03	.83–.92	.80	.04	.73–.85	ns
SSP	Left	Absolute EP	Pre	.83	.03	.78–.87	.56	.03	.51–.60	ns
	Right	Absolute EP	Pre	.49	.03	.44–.52	.65	.04	.58–.70	ns
	Left	Absolute EP	Post	.84	.02	.80–.87	.60	.08	.49–.73	ns
	Right	Absolute EP	Post	.73	.05	.63–.80	.69	.05	.60–.76	ns
	Left	Normalized EP	Post	.70	.04	.63–.76	.53	.10	.34–.65	ns
	Right	Normalized EP	Post	.40	.06	.25–.48	.53	.09	.40–.66	ns
	Left	ITPC	Post	.90	.02	.85–.93	.71	.05	.59–.78	ns
	Right	ITPC	Post	.69	.04	.62–.76	.78	.06	.64–.88	ns

SD = standard deviation; EP = evoked power; ITPC = inter-trial phase coherence; SSP = signal-space projection; Pre = pre-stimulus window (−200–0 ms); Post = post-stimulus window (200–500 ms). Electrode data taken from peak gamma-band electrode (FCz).
**p<0.01.
doi:10.1371/journal.pone.0085748.t002

[36,84]. The current results suggest that the harmonic responses seen here (at 80 Hz) do show between-session reliability, although perhaps not to the same extent as the response to the fundamental stimulus (40 Hz) (see Figure 3).

Method 2: Signal-space projection

Figure 4 shows time-frequency plots of the grand-averaged evoked power and ITPC for the signal-space projection method for the click train stimuli. The click train stimuli appeared to produce a greater ASSR (evoked power and ITPC), but no significant between-task differences (white noise stimuli vs. click stimuli) survived multiple comparison correction, with the exception of left hemisphere ITPC. In the left hemisphere, the white noise task showed significantly greater ITPC compared to the click train task in the earlier, transient gamma-band response, from 42.5 Hz–52.5 Hz from 40–100 ms ($p<0.05$, FDR-corrected). Conversely, the click train task showed significantly greater ITPC compared to the white noise task in two small areas of the steady-state response, with one time-frequency bin at 32.5 Hz/200 ms and another at 80 Hz/400 ms ($p<0.05$, FDR-corrected).

Table 3. Correlation values (Pearson's r) between sessions 1 and 2 for the baseline normalized auditory steady-state response (40 Hz, 200–500 ms): Fourier analyses.

		Click Train		White Noise		CT vs. WN
Method	**Measure**	**r**	**p**	**r**	**p**	**p**
Electrode	FCz Total Power	.73	<.001	.32	.187	ns
SSP	Left Total Power	.42	.074	.53	.020	ns
	Right Total Power	.75	<.001	.61	.006	ns

SD = standard deviation; SSP = signal-space projection; CT = click train; WN = white noise. Electrode data taken from peak gamma-band electrode (FCz). The correlations reported are for the ratios of post-stimulus/pre-stimulus power at 40 Hz.
doi:10.1371/journal.pone.0085748.t003

Means for the absolute 40 Hz response in both the pre-stimulus (−200–0 ms) and post-stimulus (200–500 ms) windows are shown in Figure 2, for both the time-frequency and Fourier transformed data. These data demonstrate significantly increased right hemisphere 40 Hz power to the click train stimuli compared to white noise stimuli in the window of the steady-state response (200–500 ms) for session 1 (TFT: $p<.001$; FFT: $p=.002$). The same relationship, albeit only marginally significant, is observed for session 2 (TFT: $p=.070$; FFT: $p=.057$). Additionally, the mean response at 40 Hz for both time-frequency and Fourier analyses was significantly greater in the left hemisphere as compared to the right hemisphere for both the white noise task (session 1, pre-and post-stimulus windows: $p<.01$ for both TFT and FFT; session 2, pre-stimulus window: $p<.01$ for both TFT and FFT; post-stimulus window: $p<0.05$ for TFT) and the click train task (session 1, pre-stimulus window: $p<.01$ for both TFT and FFT; session 2, pre-stimulus window: $p<0.05$ for both TFT and FFT). As with the sensor-space method, a harmonic response can be seen at 80 Hz.

The signal-to-noise ratio (SNR) for the ASSR (40 Hz, 200–500 ms) was calculated for each channel (left and right), across sessions (Table 1). As with the sensor-level analysis, SNR for the click train stimuli was significantly better than that for the white noise task. SNR for the peak 40 Hz channel in the sensor-level analysis (FCz) was similar to that seen for SSP. However, in the right hemisphere, SNR was significantly greater for the SSP approach compared to the sensor-level approach for both click train and white noise stimuli ($p<.001$). In the left hemisphere, SNR was also significantly greater for the SSP compared to sensor-level method for the click train stimuli ($p=.031$), but this was not significant for the white noise stimuli. The same was seen for the Fourier transform analysis, with increased SNR observed for the SSP compared to sensor-level method for right ($p=.015$) and left ($p=.003$) hemisphere for the click train task, and right hemisphere for the white noise task ($p=.001$). SNR for the right hemisphere was greater than that for the left hemisphere, in both time-frequency and Fourier analyses.

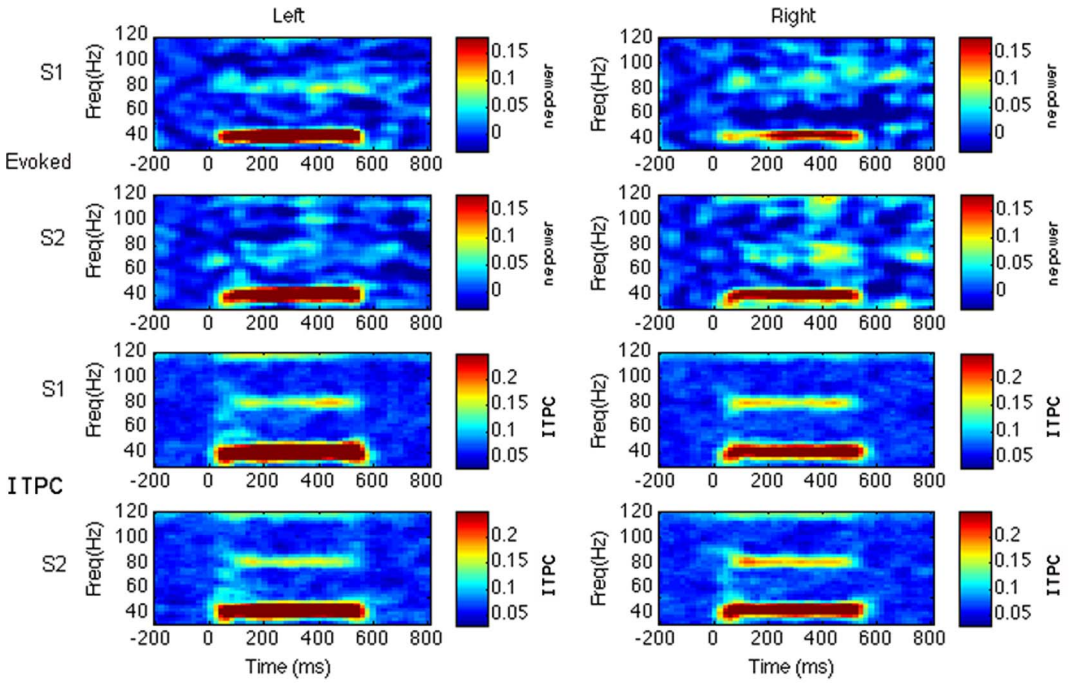


Figure 4. Example of grand averaged data. Time-frequency representations of grand-averaged evoked activity (normalized to baseline) and inter-trial phase coherence (ITPC) in response to click train stimuli for session 1 (S1) and session 2 (S2), for signal-space projected data for the left and right hemisphere. nepower = normalized evoked power.
doi:10.1371/journal.pone.0085748.g004

The SSP analysis also suggested ITPC to be more reliable between sessions than the evoked response, for both tasks. There were no time-frequency bins surviving multiple comparison correction ($p<0.05$, FDR-corrected) for the evoked response for either task with this method, while ITPC showed significant between-session correlations in the area of the ASSR (40 Hz, 200–500 ms) for both tasks, $p<0.05$, FDR-corrected. As with the sensor-level method, this appears to be more evident for click stimuli compared to white noise stimuli. However, direct comparisons of mean correlation coefficients at 40 Hz from 200–500 ms between (a) ITPC and evoked responses and (b) click train and white noise stimuli, did not find reliability to significantly differ between measure or stimulus type.

Alpha power

No significant differences in alpha power (8–12 Hz, measured at Oz) were found between the first 60 seconds (M = 1.40, SEM = .38) and the last 60 seconds (M = 1.60, SEM = .51) of session 1 for the white noise task. Similarly, there were no significant differences between the first and last 60 seconds of session 2 for the white noise task (first: M = 1.41, SEM = .59; last: M = 1.25, SEM = .46) or between the first and last 60 seconds of either session for the click train task (session 1, first: M = 1.26, SEM = .46; session 1, last: M = 1.42, SEM = .47; session 2, first: M = 1.18, SEM = .52; session 2, last: M = 1.03, SEM = .45). There were no significant differences in either the first 60 seconds or the last 60 seconds of recording within each session observed between tasks (white noise vs. click), nor were there significant differences in the change in alpha power from session 1 to session 2 between tasks. Furthermore, no significant differences in alpha power during the first and last 60 seconds of recording were observed between sessions (session 1 vs. session 2).

Discussion

Overall, this study found the auditory steady-state response (ASSR) to be significantly correlated between sessions spaced one week apart, suggesting good test-retest reliability of the response. However, this appears to be more evident for inter-trial phase coherence (ITPC) than for evoked power. The current findings of between-session reliability in the ASSR correspond well with a preliminary study by Jacobson (n = 6) that measured *transient* evoked gamma-band responses to tone stimuli. This study found the amplitude of the early peak 40 Hz response to be significantly correlated between sessions spaced one month apart [62]. The ASSR has been found to be abnormal in a number of patient populations, including autism [20], schizophrenia [18,21–26], and bipolar disorder [19,27,28]. However, there is a dearth of information on the reliability of this response. For future applicability to these patient populations, it is important to first establish the reliability of this response and its various measures (e.g., power, ITPC) in a healthy population, as was the aim of the current study.

ITPC was significantly correlated between sessions for both stimuli studied (white noise and click train) and for both analysis methods used (sensor-level and signal-space projection). While ASSR evoked power showed reliability between sessions, this did not survive multiple comparison correction in the signal-space projection analysis, and only a few voxels in select channels survived multiple comparison correction in the sensor-level analysis. Given that ITPC is amplitude-independent and the evoked response is not, making it more susceptible to noise, it is not surprising that ITPC may be more reliable between sessions. However, when directly comparing the mean correlation coefficient at 40 Hz, no significant differences were observed between ITPC and evoked power.

Across both analytical methods, the ASSR to click train stimuli was larger and appeared to be more reliable across sessions compared to the response to white noise stimuli. The reliability of the average 40 Hz normalized evoked response between 200–500 ms (ASSR) was significantly greater for click train stimuli compared to modulated white noise stimuli for the sensor-level analysis. It could be that the more rapid perceptual transition (i.e., on/off) of the clicks is more salient than the sine wave transition in the white noise stimuli, in much the same way that visual contrast is higher in square wave, compared to sine wave gratings [85,86]. That the strength and reliability of the ASSR was found to differ between stimuli in the current study is not surprising given that previous studies have also found the type of auditory stimulus to influence the size of the response [36–38]. Results across the two different analytical methods used (sensor-level and signal-space projection) were very much in agreement. Both methods suggested ITPC may be more reliable than the evoked response, although this is speculative. Furthermore, both methods found click train stimuli to elicit larger and seemingly more reliable steady-state responses compared to white noise stimuli. This was seen in both time-frequency transformed data and Fourier transformed data. This is encouraging for drawing conclusions across multiple studies, as it suggests results using separate analytical methods are comparable.

In the signal-space projection (SSP) analysis, across both tasks, a greater ASSR was seen in the left compared to right hemisphere. It is unlikely that this is due to variation in SNR between the hemispheres, as the right hemisphere demonstrated greater SNR compared to the left hemisphere. Greater SNR in right compared to left hemisphere has also been shown in MEG data [87]. SNR for the click train stimuli was better than that for the white noise task, which could perhaps explain some of the differences in power and reliability between the two tasks. Between the two methods (sensor-level and SSP), the signal-to-noise ratio of the ASSR (40 Hz, 200–500 ms) was similar, but was significantly improved in the right hemisphere for SSP compared to the sensor-level analysis. Of note, in the sensor-level analysis, data from FCz combined activity from left and right hemispheres, whereas in the signal-space projection analysis, data are separately derived for left and right hemispheres using dipoles in auditory cortex. Previous studies have also reported signal-space projection methods to result in a high SNR [36,74]. One of the challenges of EEG is enhancing the brain signal of interest while reducing the amount of noise in the data. Signal-space projection is a method of spatially filtering the data to separate out the brain activity of interest [74,88,89]. Prior research applying dipole analysis techniques to improve auditory ERP reliability also suggests the potential for this approach [63]. SSP also allows a specific area of interest to be chosen as the focus for analyses (i.e., auditory cortex in this case), which could make results more readily interpretable than those from a sensor-level analysis.

While the current study found the ASSR to be robust across sessions spaced one week apart, it remains to be seen if this response will be consistent across longer periods of time. Given that Jacobson's preliminary study [62] found peak *transient* gamma-band amplitude to be reliable across sessions spaced one month apart, it is anticipated that the *steady-state* response will show stability over time periods longer than one week. However, additional studies are needed to confirm this. Because the ASSR is increasingly being investigated as an endophenotype in various disorders, it will also be important to establish the reliability of this response in these patient populations. It could be that reliability of the response is different in various clinical populations compared to healthy controls. However, establishing the reliability of the ASSR in healthy populations is an important first step.

The current study focused on reliability of the ASSR in response to click train and white noise stimuli. While these are commonly used stimuli, particularly in the literature assessing the ASSR as a biomarker in psychiatric disorders [18–28], there are other methods of eliciting the ASSR, such as amplitude-modulated sine waves. Future studies should address the reliability of responses elicited by other stimuli than those used in the current study. In addition, a possible limitation of the current study is that the order of stimulus presentation was not counterbalanced. That is, all participants first completed the white noise task, followed by the click train task. The goal of the current study was not to identify order effects, but future studies could include a larger sample size to assess these potential effects. Because of the passive task nature, we used alpha power as a proxy measure of alertness to ascertain if there were systematic differences between sessions or tasks. Alpha power did not differ between the first and last minute of the recording within a session, suggesting that subjects were able to maintain their alertness during tasks. Additionally, no differences in alpha power were observed between sessions (session 1 vs. session 2) or between tasks (click train vs. white noise).

We found that the ASSR is consistent across recording sessions, suggesting that it is reliable over relatively short intervals. However, given that the stability of the response between sessions for evoked activity may not be as robust as for ITPC, and that consistency varied depending on stimulus type, this must be taken into consideration during experimental design. The current findings suggest that click train stimuli elicit a more reliable estimation of the ASSR than do white noise stimuli, perhaps due to the observed higher signal-to-noise ratio in that condition. Finally, we found that signal-space projection and sensor-based analysis methods elicited similar results, although the signal-to-noise ratio was higher for the signal-space projected data, consistent with previous research.

Supporting Information

Figure S1 Example of grand average for all channels for sensor-level method. Time-frequency representations of grand-averaged evoked activity (normalized to baseline) and inter-trial phase coherence (ITPC) in response to click train stimuli for session 1 (S1) and session 2 (S2), for all channels.
(TIF)

Figure S2 Correlation results for all channels for sensor-level method. Correlation results between sessions 1 and 2 for inter-trial phase coherence (ITPC) and evoked activity for white noise stimuli (A) and click train stimuli (B) for all channels. Each individual plot shows correlations that are significant following multiple comparison correction (FDR, $q = 0.05$; green = not significant, red = significant).
(TIF)

Author Contributions

Conceived and designed the experiments: DCR. Performed the experiments: KLM SES AMC STS AW. Analyzed the data: KLM AMC STS. Contributed reagents/materials/analysis tools: DCR. Wrote the paper: KLM DCR.

References

1. Basar E, Basar-Eroglu C, Karakas S, Schurmann M (2001) Gamma, alpha, delta, and theta oscillations govern cognitive processes. Int J Psychophysiol 39: 241–248.
2. Ward LM (2003) Synchronous neural oscillations and cognitive processes. Trends Cogn Sci 7: 553–559.
3. Tiitinen H, Sinkkonen J, Reinikainen K, Alho K, Lavikainen J, et al. (1993) Selective attention enhances the auditory 40-Hz transient response in humans. Nature 364: 59–60.
4. Taylor K, Mandon S, Freiwald WA, Kreiter AK (2005) Coherent oscillatory activity in monkey area v4 predicts successful allocation of attention. Cereb Cortex 15: 1424–1437.
5. Lakatos P, Karmos G, Mehta AD, Ulbert I, Schroeder CE (2008) Entrainment of neuronal oscillations as a mechanism of attentional selection. Science 320: 110–113.
6. Tallon-Baudry C, Bertrand O, Peronnet F, Pernier J (1998) Induced gamma-band activity during the delay of a visual short-term memory task in humans. J Neurosci 18: 4244–4254.
7. Pipa G, Stadtler ES, Rodriguez EF, Waltz JA, Muckli LF, et al. (2009) Performance- and stimulus-dependent oscillations in monkey prefrontal cortex during short-term memory. Front Integr Neurosci 3: 25.
8. Pantev C, Makeig S, Hoke M, Galambos R, Hampson S, et al. (1991) Human auditory evoked gamma-band magnetic fields. Proc Natl Acad Sci U S A 88: 8996–9000.
9. Pantev C, Elbert T, Makeig S, Hampson S, Eulitz C, et al. (1993) Relationship of transient and steady-state auditory evoked fields. Electroencephalogr Clin Neurophysiol 88: 389–396.
10. Gray CM, Konig P, Engel AK, Singer W (1989) Oscillatory responses in cat visual cortex exhibit inter-columnar synchronization which reflects global stimulus properties. Nature 338: 334–337.
11. Singer W (1999) Neuronal synchrony: a versatile code for the definition of relations? Neuron 24: 49–65, 111–125.
12. Pulvermuller F, Eulitz C, Pantev C, Mohr B, Feige B, et al. (1996) High-frequency cortical responses reflect lexical processing: an MEG study. Electroencephalogr Clin Neurophysiol 98: 76–85.
13. Ihara A, Hirata M, Sakihara K, Izumi H, Takahashi Y, et al. (2003) Gamma-band desynchronization in language areas reflects syntactic process of words. Neurosci Lett 339: 135–138.
14. Pena M, Melloni L (2012) Brain oscillations during spoken sentence processing. J Cogn Neurosci 24: 1149–1164.
15. Tavabi K, Embick D, Roberts TP (2011) Spectral-temporal analysis of cortical oscillations during lexical processing. Neuroreport 22: 474–478.
16. Galambos R, Makeig S, Talmachoff PJ (1981) A 40-Hz auditory potential recorded from the human scalp. Proc Natl Acad Sci U S A 78: 2643–2647.
17. Ross B, Picton TW, Pantev C (2002) Temporal integration in the human auditory cortex as represented by the development of the steady-state magnetic field. Hear Res 165: 68–84.
18. Kwon JS, O'Donnell BF, Wallenstein GV, Greene RW, Hirayasu Y, et al. (1999) Gamma frequency-range abnormalities to auditory stimulation in schizophrenia. Arch Gen Psychiatry 56: 1001–1005.
19. Maharajh K, Abrams D, Rojas DC, Teale P, Reite ML (2007) Auditory steady state and transient gamma band activity in bipolar disorder. Int Cong Ser 1300: 707–710.
20. Wilson TW, Rojas DC, Reite ML, Teale PD, Rogers SJ (2007) Children and adolescents with autism exhibit reduced MEG steady-state gamma responses. Biol Psychiatry 62: 192–197.
21. Spencer KM, Salisbury DF, Shenton ME, McCarley RW (2008) Gamma-band auditory steady-state responses are impaired in first episode psychosis. Biol Psychiatry 64: 369–375.
22. Lee KH, Williams LM, Haig A, Goldberg E, Gordon E (2001) An integration of 40 Hz gamma and phasic arousal: novelty and routinization processing in schizophrenia. Clin Neurophysiol 112: 1499–1507.
23. Brenner CA, Sporns O, Lysaker PH, O'Donnell BF (2003) EEG synchronization to modulated auditory tones in schizophrenia, schizoaffective disorder, and schizotypal personality disorder. Am J Psychiatry 160: 2238–2240.
24. Lee KH, Williams LM, Breakspear M, Gordon E (2003) Synchronous gamma activity: a review and contribution to an integrative neuroscience model of schizophrenia. Brain Res Brain Res Rev 41: 57–78.
25. Light GA, Hsu JL, Hsieh MH, Meyer-Gomes K, Sprock J, et al. (2006) Gamma band oscillations reveal neural network cortical coherence dysfunction in schizophrenia patients. Biol Psychiatry 60: 1231–1240.
26. Uhlhaas PJ, Haenschel C, Nikolic D, Singer W (2008) The role of oscillations and synchrony in cortical networks and their putative relevance for the pathophysiology of schizophrenia. Schizophr Bull 34: 927–943.
27. O'Donnell BF, Hetrick WP, Vohs JL, Krishnan GP, Carroll CA, et al. (2004) Neural synchronization deficits to auditory stimulation in bipolar disorder. Neuroreport 15: 1369–1372.
28. Oda Y, Onitsuka T, Tsuchimoto R, Hirano S, Oribe N, et al. (2012) Gamma band neural synchronization deficits for auditory steady state responses in bipolar disorder patients. PLoS One 7: e39955.
29. Hong LE, Summerfelt A, McMahon R, Adami H, Francis G, et al. (2004) Evoked gamma band synchronization and the liability for schizophrenia. Schizophr Res 70: 293–302.
30. Rass O, Forsyth JK, Krishnan GP, Hetrick WP, Klaunig MJ, et al. (2012) Auditory steady state response in the schizophrenia, first-degree relatives, and schizotypal personality disorder. Schizophr Res 136: 143–149.
31. Rojas DC, Teale PD, Maharajh K, Kronberg E, Youngpeter K, et al. (2011) Transient and steady-state auditory gamma-band responses in first-degree relatives of people with autism spectrum disorder. Mol Autism 2: 11.
32. Stapells DR, Linden D, Suffield JB, Hamel G, Picton TW (1984) Human auditory steady state potentials. Ear Hear 5: 105–113.
33. Rees A, Green GG, Kay RH (1986) Steady-state evoked responses to sinusoidally amplitude-modulated sounds recorded in man. Hear Res 23: 123–133.
34. Picton TW, Dauman R, Aran JM (1987) Responses evoked in "steady state" in man by means of a sinusoidal frequency modulation. J Otolaryngol 16: 140–145.
35. Cohen LT, Rickards FW, Clark GM (1991) A comparison of steady-state evoked potentials to modulated tones in awake and sleeping humans. J Acoust Soc Am 90: 2467–2479.
36. Ross B, Borgmann C, Draganova R, Roberts LE, Pantev C (2000) A high-precision magnetoencephalographic study of human auditory steady-state responses to amplitude-modulated tones. J Acoust Soc Am 108: 679–691.
37. John MS, Dimitrijevic A, Picton TW (2003) Efficient stimuli for evoking auditory steady-state responses. Ear Hear 24: 406–423.
38. Picton TW, John MS, Dimitrijevic A, Purcell D (2003) Human auditory steady-state responses. Int J Audiol 42: 177–219.
39. Lewis DA, Hashimoto T, Volk DW (2005) Cortical inhibitory neurons and schizophrenia. Nat Rev Neurosci 6: 312–324.
40. Vohs JL, Chambers RA, Krishnan GP, O'Donnell BF, Berg S, et al. (2010) GABAergic modulation of the 40 Hz auditory steady-state response in a rat model of schizophrenia. Int J Neuropsychopharmacol 13: 487–497.
41. Bartos M, Vida I, Jonas P (2007) Synaptic mechanisms of synchronized gamma oscillations in inhibitory interneuron networks. Nat Rev Neurosci 8: 45–56.
42. Brenner CA, Krishnan GP, Vohs JL, Ahn WY, Hetrick WP, et al. (2009) Steady state responses: electrophysiological assessment of sensory function in schizophrenia. Schizophr Bull 35: 1065–1077.
43. Muthukumaraswamy SD, Singh KD, Swettenham JB, Jones DK (2010) Visual gamma oscillations and evoked responses: variability, repeatability and structural MRI correlates. Neuroimage 49: 3349–3357.
44. Hussman JP (2001) Suppressed GABAergic inhibition as a common factor in suspected etiologies of autism. J Autism Dev Disord 31: 247–248.
45. Pizzarelli R, Cherubini E (2011) Alterations of GABAergic signaling in autism spectrum disorders. Neural Plast 2011: 297153.
46. Coghlan S, Horder J, Inkster B, Mendez MA, Murphy DG, et al. (2012) GABA system dysfunction in autism and related disorders: from synapse to symptoms. Neurosci Biobehav Rev 36: 2044–2055.
47. Gonzalez-Burgos G, Lewis DA (2008) GABA neurons and the mechanisms of network oscillations: implications for understanding cortical dysfunction in schizophrenia. Schizophr Bull 34: 944–961.
48. Benes FM, Berretta S (2001) GABAergic interneurons: implications for understanding schizophrenia and bipolar disorder. Neuropsychopharmacology 25: 1–27.
49. Brady RO, Jr., McCarthy JM, Prescot AP, Jensen JE, Cooper AJ, et al. (2013) Brain gamma-aminobutyric acid (GABA) abnormalities in bipolar disorder. Bipolar Disord [Epub ahead of print].
50. Segalowitz SJ, Barnes KL (1993) The reliability of ERP components in the auditory oddball paradigm. Psychophysiology 30: 451–459.
51. Tervaniemi M, Lehtokoski A, Sinkkonen J, Virtanen J, Ilmoniemi RJ, et al. (1999) Test-retest reliability of mismatch negativity for duration, frequency and intensity changes. Clin Neurophysiol 110: 1388–1393.
52. Raikkonen K, Birkas E, Horvath J, Gervai J, Winkler I (2003) Test-retest reliability of auditory ERP components in healthy 6-year-old children. Neuroreport 14: 2121–2125.
53. Gaspar CM, Rousselet GA, Pernet CR (2011) Reliability of ERP and single-trial analyses. Neuroimage 58: 620–629.
54. Cassidy SM, Robertson IH, O'Connell RG (2012) Retest reliability of event-related potentials: evidence from a variety of paradigms. Psychophysiology 49: 659–664.
55. Gasser T, Bacher P, Steinberg H (1985) Test-retest reliability of spectral parameters of the EEG. Electroencephalogr Clin Neurophysiol 60: 312–319.
56. Salinsky MC, Oken BS, Morehead L (1991) Test-retest reliability in EEG frequency analysis. Electroencephalogr Clin Neurophysiol 79: 382–392.
57. McEvoy LK, Smith ME, Gevins A (2000) Test-retest reliability of cognitive EEG. Clin Neurophysiol 111: 457–463.
58. Nikulin VV, Brismar T (2004) Long-range temporal correlations in alpha and beta oscillations: effect of arousal level and test-retest reliability. Clin Neurophysiol 115: 1896–1908.
59. Keil A, Stolarova M, Heim S, Gruber T, Muller MM (2003) Temporal stability of high-frequency brain oscillations in the human EEG. Brain Topogr 16: 101–110.

60. Hoogenboom N, Schoffelen JM, Oostenveld R, Parkes LM, Fries P (2006) Localizing human visual gamma-band activity in frequency, time and space. Neuroimage 29: 764–773.
61. Frund I, Schadow J, Busch NA, Korner U, Herrmann CS (2007) Evoked gamma oscillations in human scalp EEG are test-retest reliable. Clin Neurophysiol 118: 221–227.
62. Jacobson GP, McCaslin DL, Smith B, Elisevich K, Mishler P (1999) Test-retest stability and short-term habituation of the N1 and gamma band response. J Am Acad Audiol 10: 211–218.
63. Cardenas VA, Gerson J, Fein G (1993) The reliability of P50 suppression as measured by the conditioning/testing ratio is vastly improved by dipole modeling. Biol Psychiatry 33: 335–344.
64. First MB, Gibbon M, Spitzer RL, Williams JBW, Benjamin LS (1991) Structured Clinical Interview for DSM-IV Screen Patient Questionnaire-Extended. Toronto, ON: Multi-Health Systems.
65. Ross B, Picton TW, Herdman AT, Pantev C (2004) The effect of attention on the auditory steady-state response. Neurol Clin Neurophysiol 2004: 22.
66. Skosnik PD, Krishnan GP, O'Donnell BF (2007) The effect of selective attention on the gamma-band auditory steady-state response. Neurosci Lett 420: 223–228.
67. Nuwer MR, Comi G, Emerson R, Fuglsang-Frederiksen A, Guerit JM, et al. (1998) IFCN standards for digital recording of clinical EEG. International Federation of Clinical Neurophysiology. Electroencephalogr Clin Neurophysiol 106: 259–261.
68. Berg P, Scherg M (1994) A multiple source approach to the correction of eye artifacts. Electroencephalogr Clin Neurophysiol 90: 229–241.
69. Ille N, Berg P, Scherg M (1997) A spatial components method for continuous artifact correction in EEG and MEG. Biomed Tech 42: 80–83.
70. Ille N, Berg P, Scherg M (2002) Artifact correction of the ongoing EEG using spatial filters based on artifact and brain signal topographies. J Clin Neurophysiol 19: 113–124.
71. Papp N, Ktonas P (1977) Critical evaluation of complex demodulation techniques for the quantification of bioelectrical activity. Biomed Sci Instrum 13: 135–145.
72. Hoechstetter K, Bornfleth H, Weckesser D, Ille N, Berg P, et al. (2004) BESA source coherence: a new method to study cortical oscillatory coupling. Brain Topogr 16: 233–238.
73. Scherg M, Von Cramon D (1986) Evoked dipole source potentials of the human auditory cortex. Electroencephalogr Clin Neurophysiol 65: 344–360.
74. Scherg M (1990) Fundamentals of dipole source potential analysis. In: Grandori F, Hoke M, Romani GL, Auditory Evoked Magnetic Fields and Electrical Potentials (Advances in Audiology). Switzerland: Karger. pp. 40–69.
75. Scherg M, Berg P (1996) New concepts of brain source imaging and localization. Electroencephalogr Clin Neurophysiol Suppl 46: 127–137.
76. Oostenveld R, Fries P, Maris E, Schoffelen JM (2011) FieldTrip: open source software for advanced analysis of MEG, EEG, and invasive electrophysiological data. Comput Intell Neurosci 2011: 156869.
77. Tallon-Baudry C, Bertrand O, Delpuech C, Pernier J (1996) Stimulus specificity of phase-locked and non-phase-locked 40 Hz visual responses in human. J Neurosci 16: 4240–4249.
78. Roach BJ, Mathalon DH (2008) Event-related EEG time-frequency analysis: an overview of measures and an analysis of early gamma band phase locking in schizophrenia. Schizophr Bull 34: 907–926.
79. Benjamini Y, Hochberg Y (1995) Controlling the false discovery rate: a practical and powerful approach to multiple testing. JR Stastist Soc 57: 289–300.
80. Dobie RA, Wilson MJ (1993) Objective response detection in the frequency domain. Electroencephalogr Clin Neurophysiol 88: 516–524.
81. Robinson SE (1989) Theory and Properties of Lead Field Synthesis Analysis. In: Williamson SJ, Hoke M, Stroink G, Kotani M, Advances in Biomagnetism. New York: Plenum Press. pp. 599–602.
82. Teale P, Collins D, Maharajh K, Rojas DC, Kronberg E, et al. (2008) Cortical source estimates of gamma band amplitude and phase are different in schizophrenia. Neuroimage 42: 1481–1489.
83. Scherg M, Ille N, Bornfleth H, Berg P (2002) Advanced tools for digital EEG review: virtual source montages, whole-head mapping, correlation, and phase analysis. J Clin Neurophysiol 19: 91–112.
84. Heinrichs-Graham E, Wilson TW (2012) Presence of strong harmonics during visual entrainment: a magnetoencephalography study. Biol Psychol 91: 59–64.
85. Campbell FW, Robson JG (1968) Application of Fourier analysis to the visibility of gratings. J Physiol 197: 551–566.
86. Gowdy PD, Stromeyer CF, 3rd, Kronauer RE (1999) Facilitation between the luminance and red-green detection mechanisms: enhancing contrast differences across edges. Vision Res 39: 4098–4112.
87. Ross B, Herdman AT, Pantev C (2005) Right hemispheric laterality of human 40 Hz auditory steady-state responses. Cereb Cortex 15: 2029–2039.
88. Tesche CD, Uusitalo MA, Ilmoniemi RJ, Huotilainen M, Kajola M, et al. (1995) Signal-space projections of MEG data characterize both distributed and well-localized neuronal sources. Electroencephalogr Clin Neurophysiol 95: 189–200.
89. Uusitalo MA, Ilmoniemi RJ (1997) Signal-space projection method for separating MEG or EEG into components. Med Biol Eng Comput 35: 135–140.

frontiers in Neurology

ORIGINAL RESEARCH
published: 27 November 2017
doi: 10.3389/fneur.2017.00615

Structural Covariance of Sensory Networks, the Cerebellum, and Amygdala in Autism Spectrum Disorder

*Garrett J. Cardon[1], Susan Hepburn[2] and Donald C. Rojas[1]**

[1] Department of Psychology, Colorado State University, Fort Collins, CO, United States, [2] Department of Human Development and Family Studies, Colorado State University, Fort Collins, CO, United States

Sensory dysfunction is a core symptom of autism spectrum disorder (ASD), and abnormalities with sensory responsivity and processing can be extremely debilitating to ASD patients and their families. However, relatively little is known about the underlying neuroanatomical and neurophysiological factors that lead to sensory abnormalities in ASD. Investigation into these aspects of ASD could lead to significant advancements in our general knowledge about ASD, as well as provide targets for treatment and inform diagnostic procedures. Thus, the current study aimed to measure the covariation of volumes of brain structures (i.e., structural magnetic resonance imaging) that may be involved in abnormal sensory processing, in order to infer connectivity of these brain regions. Specifically, we quantified the structural covariation of sensory-related cerebral cortical structures, in addition to the cerebellum and amygdala by computing partial correlations between the structural volumes of these structures. These analyses were performed in participants with ASD (n = 36), as well as typically developing peers (n = 32). Results showed decreased structural covariation between sensory-related cortical structures, especially between the left and right cerebral hemispheres, in participants with ASD. In contrast, these same participants presented with increased structural covariation of structures in the right cerebral hemisphere. Additionally, sensory-related cerebral structures exhibited decreased structural covariation with functionally identified cerebellar networks. Also, the left amygdala showed significantly increased structural covariation with cerebral structures related to visual processing. Taken together, these results may suggest several patterns of altered connectivity both within and between cerebral cortices and other brain structures that may be related to sensory processing.

Keywords: structural covariation, autism spectrum disorder, sensory dysfunction, cerebellum, amygdala

OPEN ACCESS

Edited by:
Christian Gaser, Friedrich Schiller, Universität Jena, Germany

Reviewed by:
Jussi Tohka, University of Eastern Finland, Finland
Ralf Tepest, University Hospital of Cologne, Germany

****Correspondence:***
Donald C. Rojas
don.rojas@colostate.edu

Specialty section:
This article was submitted to Applied Neuroimaging, a section of the journal Frontiers in Neurology

Received: *07 June 2017*
Accepted: *03 November 2017*
Published: *27 November 2017*

Citation:
Cardon GJ, Hepburn S and Rojas DC (2017) Structural Covariance of Sensory Networks, the Cerebellum, and Amygdala in Autism Spectrum Disorder. Front. Neurol. 8:615. doi: 10.3389/fneur.2017.00615

INTRODUCTION

Diagnostic criteria for autism spectrum disorder (ASD) underwent revision in 2013 [DSM 5 (1)]. One major change to the criteria is that sensory dysfunction was added as a symptom area able to meet criterion B.4 (restricted and repetitive behaviors, interests, or activities), highlighting its importance as a core feature of ASD. Despite this recent recognition, as well as estimates

of the prevalence of sensory problems in ASD exceeding 90% (2–5), sensory dysfunction in ASD is poorly understood. This gap is especially notable with respect to the neurobiological underpinnings of sensory dysfunction (6). Gaining knowledge about sensory dysfunction in ASD is needed in order to devise ways to ameliorate their debilitating effects on patients and their families. Neuroimaging techniques, such as magnetic resonance imaging (MRI), can provide opportunities to better describe neurophysiologic correlates of sensory dysfunction in humans with ASD. The current study aimed to investigate anatomical relationships between cortical and subcortical structures involved in sensory processing as well as the cerebellum and amygdala as an initial step toward examining the neurobiological underpinnings of sensory dysfunction in ASD.

Changes in brain connectivity are a theme emerging across several theories of ASD [i.e., Weak Central Coherence, Predictive Coding, Reduced Sensory Precision, Temporal Binding Deficit, and Excitatory/Inhibitory Imbalance; e.g., (7–16)]. These perspectives suggest that phenotypes associated with ASD are subserved by deficits in distributed neurological networks, rather than single portions of the brain. Indeed, the available literature on the neural bases of sensory dysfunction in ASD suggests that unisensory subcortical and cortical processing, though involved, is likely not the only process contributing to abnormal sensory responsivity (17). Rather, evidence points to other, supra-modal, brain structures that may also be involved in sensory dysfunction. For example, one of the most often reported structural abnormalities in ASD is found in the cerebellum (18–24). Both Purkinje cell loss (18) and decreased cerebellar gray matter volumes (19–22, 25, 26) have consistently been shown in ASD relative to control subjects. While the cerebellum is typically thought of in terms of its role in motor function (27), the cerebellum also plays a role in both multisensory integration (24, 28) and prediction of sensory input (29). Its multisensory integration function is supported by the fact that the cerebellum receives projections from all sensory modalities and the areas of the cerebellum to which these sensory systems project often overlap (24, 30). For instance, self-motion requires integration of vestibular, visual, proprioceptive, and somatosensory information. Specifically, vestibular and proprioceptive information is combined with multiple sensory modalitys' information in the cerebellum to generate representations about head and body position, translation, and tilt, and heading direction (17). A cerebellar deficiency would therefore negatively affect responses to sensory stimuli, regardless of the modality, by hampering multisensory integration, and both the ability to anticipate sensory events and prepare appropriate response to the same.

Additionally, overstimulation perceived as threatening could be related to enhanced fear responses in ASD, which would likely be mediated by non-sensory-specific brain regions (31–33). Following this line of reasoning, the amygdala could be postulated as involved in the abnormal sensory responsivity in ASD, given its classic role in fear processing, its connections to sensory systems, and oft reported abnormalities in ASD (6, 34–36). For example, it has been shown that the degree to which the amygdala is stimulated during a sensory event predicts the extent to which that sensory experience is deemed unpleasant or threatening (34). Thus, it is plausible to hypothesize that in addition to sensory-specific cortical regions, other brain areas such as the cerebellum and amygdala may be critical to sensory dysfunction and reactivity in ASD.

Establishing the notion of distributed network involvement in sensory dysfunction necessitates measures of neural connectivity and co-activation. For instance, studies involving functional connectivity (i.e., covariation of the BOLD response between regions of interest in the brain) have shown significant differences between participants with ASD and those who were typically developing [TD (37–40)]. One of the most common functional connectivity findings reveals that local, within-region connectivity is enhanced, while long-range connections appear weakened in ASD, relative to controls, especially in the default mode network [DMN (11–13, 15, 29, 37, 41–44)]. In addition to functional connectivity, some previous reports have also shown significant differences between those with ASD and TD peers in the structural features of their brains [see Pua et al. (45) for a review]. Furthermore, the covariation of structural attributes of distinct brain regions (i.e., volume, thickness, surface area) has recently been used as a measure of connectivity (46). This type of analysis has been termed morphological connectivity, although to avoid conflating the term with more direct functional and structural metrics of connectivity, we prefer the term covariation. The assumption of morphological covariation is that regions of the brain that are connected and co-active also tend to covary in their structural characteristics. These structural relationships may be mediated by common experience-dependent plasticity or mutually trophic influences (46). A number of studies have found significant results using structural/morphological covariation as a measure of related brain regions in ASD vs. TD controls (47, 48). In fact, recently, several investigations have reported findings that support the use of morphological covariation as a means to distinguish participants with ASD from TD subjects (48). However, no study of morphological covariation in ASD has focused specifically on neural centers related to sensory processing and dysfunction, to our knowledge. Thus, the current investigation aimed to evaluate the morphological covariation between cortical regions known to be associated with sensory function, such as the temporal and occipital cortices and post-central gyrus, as well as supramodal brain areas that may be instrumental in sensory processing and dysfunction in ASD, including the cerebellum, amygdala, and language-related areas (e.g., supramarginal gyrus and caudal medial prefrontal cortex). We hypothesized that local morphological covariation would be enhanced, while long-range covariation would be decreased in individuals with ASD, compared to controls. Additionally, we predicted that structural correlations between the cerebellum and sensory cortices would be weaker in ASD compared with controls. Finally, we hypothesized that sensory cortices would exhibit stronger covariance to the amygdala in those with ASD relative to matched controls.

MATERIALS AND METHODS

Participants

Participants for the current study consisted of two groups of male participants: (1) individuals with ASD (n = 36; mean age = 18.24 years, SD = 9.9); (2) TD individuals (n = 32; mean age = 18.9 years, SD = 12.28). Ages of these groups did not differ significantly [$t(66) = -0.26$, $p = 0.80$]. ASD subjects were diagnosed using a convergence of meeting criteria on (1) the Autism Diagnostic Observation Schedule—Generic [ADOS-G (49)], (2) the Autism Diagnostic Interview Revised (ADI™-R) (50) or Social Communication Questionnaire [SCQ (51)], and (3) confirmation of the diagnosis by a clinical psychologist with expertise in ASD using a DSM-IV checklist during a clinical interview. A second psychologist reviewed case diagnostic data and independently formulated a DSM-IV diagnosis. The ASD diagnosis therefore employed DSM-IV criteria and included Autistic Disorder (n = 19), Asperger's Syndrome (n = 15), and PDD-NOS (n = 2). Agreement on ASD vs. not ASD was 100% and agreement on specific ASD sub-diagnosis was 88%. Severity of ASD symptoms was measured using the Social Responsiveness Scale, Second Edition [(52); SRS-2], a 65-item questionnaire that measures several aspects of social functioning that accurately distinguish ASD from other psychiatric disorders. As a group, those with ASD presented with a mean score of 96.79 (SD = 25.5), which is in the severe symptom range and is highly indicative of clinical diagnoses of ASD. Non-verbal IQ (Wechsler Abbreviated Scale of Intelligence) scores were available in a subset of individuals from both the ASD (n = 32) and TD (n = 27) groups and were as follows: ASD—mean IQ = 111.19, SD = 14.95; TD—mean IQ = 116.26, SD = 12.46. The ASD and TD groups did not differ significantly in non-verbal IQ ($t = -1.39$; $p = 0.25$). Individuals were excluded from the study if they: (1) had a known genetic etiology of ASD (e.g., Fragile X Syndrome, Tuberous Sclerosis, 15q syndrome, etc.); (2) had a full-scale IQ below 70; (3) had a history of seizure disorder; or (4) had a history of brain injury, stroke, or other neurological disorder. All participants were recruited in accordance with human subjects protection policies of the Colorado Multiple Institutional Review Board (COMIRB) of the University of Colorado Denver Anschutz Medical Campus, where MRI scanning took place.

MRI Acquisition

The T1-weighted structural MRI scan data used in the current study were obtained from participants in an NIH-funded study to DCR concerning magnetoencephalographic brain activity in ASD, and as such were not specifically acquired to answer questions of sensory processing abnormality. The data were acquired using a 3.0 T GE Signa HDx long-bore MR scanner (General Electric Hardware, WI, USA) together with a GE 8-channel phased-array head coil. In order to minimize participant motion and to improve compliance, subjects were allowed to watch and listen to a movie through MR compatible goggles and head phones (Resonance Technology, Inc., Northridge, CA, USA). For tissue segmentation, a T1-weighted sequence was acquired using a 3D inversion recovery, fast, spoiled gradient echo (IR-SPGR) technique (matrix = 256^2, FOV 22 cm, TR/TE/TI = 10/3/450 ms, NEX = 1). MR acquisitions resulted in 138, 1.2 mm thick axial slices with an in-plane resolution of 0.86 mm^2.

Structural Covariation and Statistical Analysis

Volumetric measurements for the sensory and supramodal structures of interest were calculated using the Freesurfer 5.3 image analysis suite (http://surfer.nmr.mgh.harvard.edu/). Freesurfer has been used widely to perform automatic volumetric calculation and has shown good test–retest reliability across manufacturers of MR scanners, as well as field strengths (53, 54). The details behind the extraction of volumetric data have been well described in previous publications (53–66). In general, cortical surface reconstruction was performed *via* the following preprocessing steps: intensity normalization, skull stripping, pial surface generation, and use of triangular tessellation to generate a white/gray matter boundary [as in Tanabe et al. (67)]. Manual edits were made to volumes and surfaces as needed to correct issues remaining after automated processes.

Fifty-four anatomically distinct brain regions were included in the volumetric analysis (68). In general, the structures consisted of subdivisions of the frontal, temporal, occipital, and parietal cortices, as well as the amygdala. In addition, information regarding the volumes of the cerebellar hemispheres and seven functionally distinct cerebellar networks was extracted from the structural MRI scan by applying a cerebellar network template (69, 70) to participants' scans. Once obtained, volumetric data were entered into the SPSS software package and Matlab for statistical analysis [(71); version 23; The Mathworks, version 2014b with Statistical Toolbox]. In order to compare volumetric data between groups, a general linear model was formed with structural volumes as the dependent variables, diagnosis as the independent variable, and intracranial volume as a covariate. Findings from this test were subjected to multiple comparisons adjustment using a false discovery rate (FDR) adjustment procedure [$q = 0.1$ (72)]. Following this between groups analysis, partial (i.e., removing the effects of intracranial volume and age) correlation coefficients were permuted (randomized labeling exchanges between subjects) between all structure pairs (10,000 permutations for each pair). Non-parametric p-values were then obtained by taking the number of permuted partial correlation coefficients higher than the actual partial correlation for each pair by the total number of permutations (absolute values of the coefficients were used in this procedure to yield two-tailed results). These non-parametric partial correlation p-values were then subjected to multiple comparisons adjustment by FDR.

Finally, between group differences in the correlation data were assessed for all structure pairings as follows: (1) a Fisher's r to z transform was computed to obtain z-scores, (2) z-scores were compared according to the formula from Cohen and Cohen (73), and (3) p-values were obtained *via* permutations of the group membership (10,000 permutations each with randomized group label exchanges).

RESULTS

Between Group Structural Volumetric Comparisons

All volume statistics included intracranial volume as covariates to account for general variability of brain size. Between groups comparison of absolute structural volumes revealed that several structures differed significantly between the ASD and TD groups. For example, the left and right transverse temporal volumes were significantly larger in the ASD vs. the TD group [left: $F(1, 54) = 13.73$; $q = 0.00$; right: $F(1, 54) = 10.99$; $q = 0.03$]. On the other hand, the right banks of the superior temporal sulcus was significantly smaller in the ASD group [$F(1, 54) = 10.91$; $q = 0.03$]. Also, the nucleus accumbens from both the left and right hemispheres were both significantly smaller overall in the participants with ASD [left: $F(1, 54) = 7.77$; $q = 0.08$; right: $F(1, 54) = 16.12$; $q = 0.00$]. Significance, mean, and SD volume values can be seen in Table S1 in Supplementary Material. Significant differences in these particular brain regions, which are highly associated with sensory processing, may be related to abnormalities in sensory function in the ASD group.

Sensory Cortical Structural Covariance

The structural (i.e., partial) correlations that remained significant following multiple comparisons correction for both the ASD and TD groups can be seen in **Figure 1**. These data reveal several notable findings with respect to the hypotheses of the current study. For instance, subjects with ASD present with few significant correlations between the right and left hemispheres compared to TD participants (i.e., inter-hemispheric covariation). In contrast, significant within hemisphere (i.e., intra-hemispheric covariation) structural correlations seem more abundant than inter-hemispheric correlations in the ASD group, especially within the right hemisphere.

Between Groups Comparison of Structural Covariation

In order to examine between group differences in structural covariation, we plotted the z-scores of the correlations that were significantly different between groups (i.e., Fisher's z transform). These data can be seen in **Figure 2**. In this figure, blue cells are indicative of correlations that were stronger in the TD group, while red cells show correlations that were stronger in the ASD group. Consistent with the above results, overall, the TD group showed significantly stronger inter-hemispheric and cerebellar cortex–functional cerebellar network correlations than the ASD group. On the other hand, the ASD participants presented with significantly more intra-hemispheric correlations.

Also germane to the current hypotheses, the functional networks of the cerebellum (69, 70) showed fewer correlations with sensory-related structures in the ASD group, vs. controls. Notably, the control group showed significant covariation between the cerebellar network associated with somatomotor function and the left pericalcarine ($z = -2.04$; $p = 0.03$), superior temporal ($z = -1.90$; $p = 0.03$), and transtemporal cortices ($z = -2.34$; $p = 0.03$). Additionally, this group exhibited several significant correlations between the dorsal attention functional cerebellar networks and visual cortices [i.e., left cuneus ($z = -2.15$;

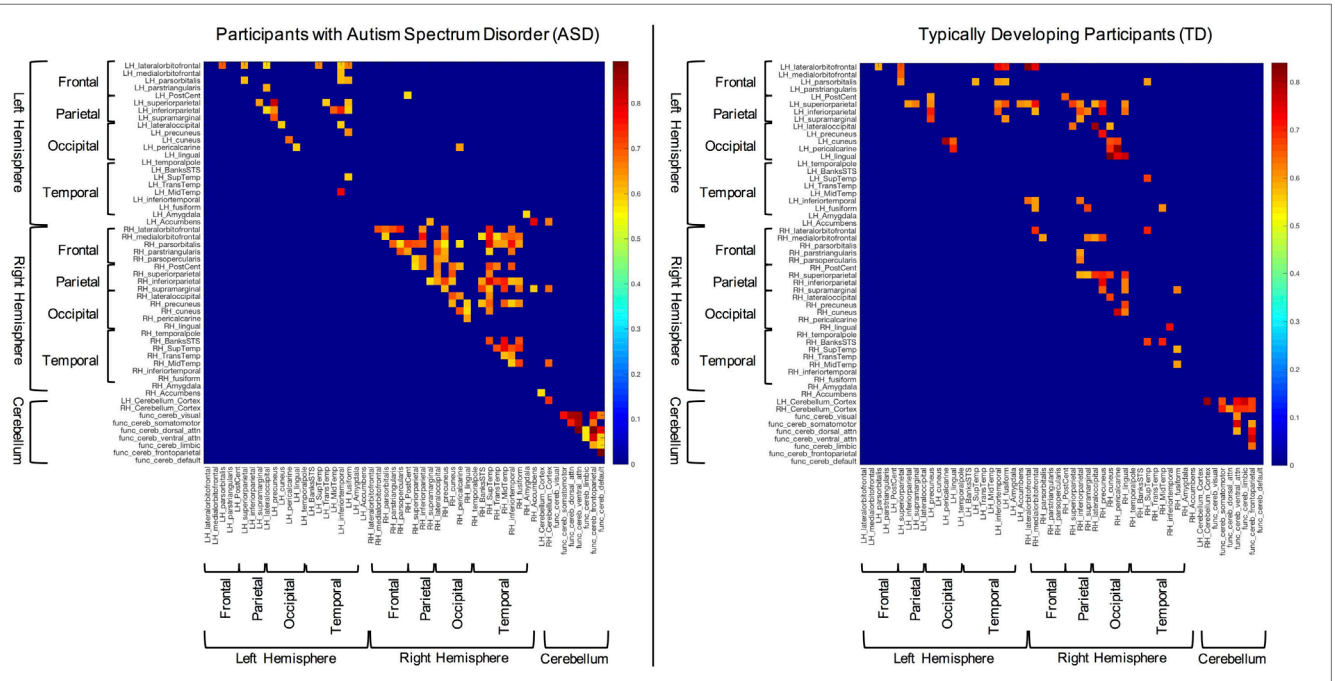


FIGURE 1 | Significant structural correlations in the autism spectrum disorder and typically developing (TD) groups (following multiple comparisons correction). Hemispheres, lobes, and cerebellum are marked with brackets for convenience.

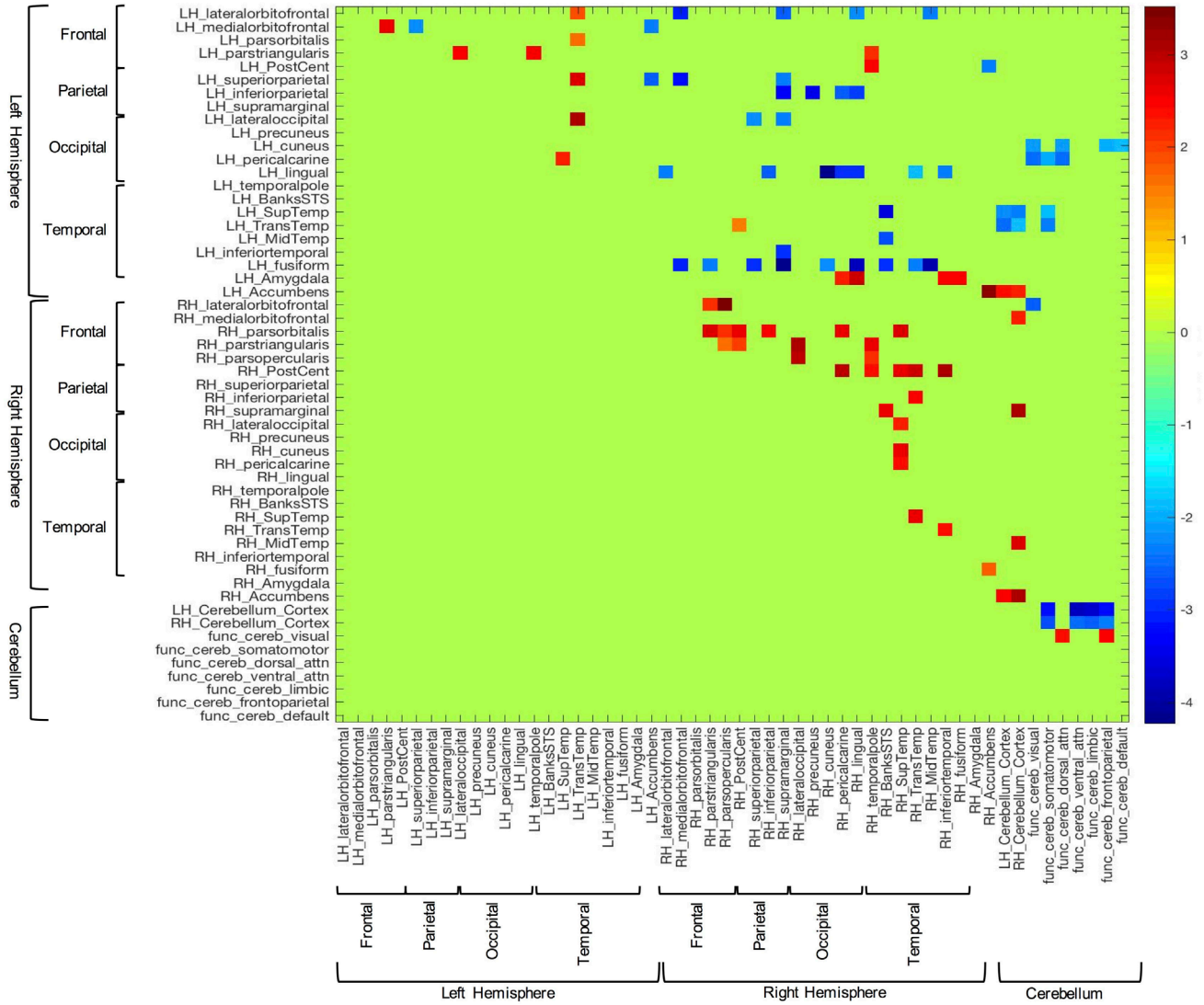


FIGURE 2 | Z-scores of structural volume correlations masked by the indices of significantly different between group correlations (corrected for multiple comparisons). Blue cells represent z-scores associated with stronger correlations in the typically developing group, while red cells correspond to stronger correlations from the autism spectrum disorder group.

$p = 0.04$) and pericalcarine cortex ($z = -2.42$; $p = 0.04$)]. In contrast, the ASD group did not show any significant correlations in the above areas.

In the between groups comparison, the covariation between the amygdala and sensory-related structures showed the opposite pattern compared to the cerebellum. That is, the TD group showed no significantly stronger correlations with the amygdala, while those with ASD showed several correlations of note. For instance, the volume of the left amygdala was more strongly correlated with several cortical areas associated with visual processing, including some highly implicated in facial processing [i.e., right pericalcarine ($z = 2.29$; $p = 0.05$), lingual ($z = 2.91$; $p = 0.03$), inferior temporal ($z = 2.45$; $p = 0.04$), and fusiform cortices ($z = 2.48$; $p = 0.04$)].

DISCUSSION

The results of the current study suggest that individuals with ASD present with altered structural volumes and covariance in brain regions that may be associated with sensory processing and reactivity, prediction, and emotion. The following findings support these notions: (i) participants with ASD exhibited larger right and left transverse temporal gyrus volumes, while these same subjects presented with smaller overall volumes of the right banks of the STS, and left and right nucleus accumbens, relative to TD participants (see Between Group Structural Volumetric Comparisons); (ii) increased covariation was seen between structural volumes of sensory-related cortices within the right and, to a lesser degree, left hemispheres of persons with ASD

vs. TD subjects. In contrast, ASD participants showed decreased covariation of structural volumes of sensory-related cortices between the right and left cerebral hemispheres, compared to the TD group (**Figures 1** and **2**); (iii) overall, the ASD group showed differences in structural covariation between the cerebellum and sensory-related cerebrum, in contrast to the TD group (**Figure 2**); (iv) the ASD group presented with a greater number of significant amygdala–sensory cortical correlations than TD peers, especially in the right hemisphere. Furthermore, the amygdalae of ASD participants showed significantly increased average structural volumetric correlations to the right occipital and temporal cortices (**Figure 2**).

Inter- vs. Intra-Hemispheric Correlations of Sensory Cortical Structures

Various studies, using both structural and functional techniques, have demonstrated altered cortical network characteristics in ASD. Probably the most common finding among these studies concerns local hyperconnectivity, with hypo-connectivity of long-range circuits (12, 13, 15, 38, 74–78). This type of result has been shown, for example, in the DMN, in which increased connectivity was seen in local network nodes, while longer-range connections running in an anterior–posterior orientation were compromised (38, 76). Additionally, decreased inter-hemispheric and cerebellar-cerebral (i.e., long-range) resting sate functional connectivity (75, 79), as well as increased right hemisphere connectivity [i.e., shorter-range (76, 80)] have been reported in ASD. Such a connectivity pattern might leave specialized information processing units isolated from other brain regions, because of the lack of global connectivity (7, 8). The results of the current study, indicating that local correlation within both cortical hemispheres was increased, coupled with decreased inter-hemispheric correlations, are consistent with the above notions. This structural covariance pattern may reflect hyperconnectivity of specialized local sensory networks and isolation of the same due to deficient inter-hemispheric connections. Within local networks, this type of finding may be related to behavioral hyper-arousal and hyper-focus on certain sensory inputs in ASD (81–83). Also, both short- and long-range sensory covariance results could be associated with symptoms of weak central coherence—another commonly reported theory in ASD (7).

One area of sensory processing that has been highly implicated in ASD is multisensory integration. That is, numerous investigators have argued that individuals with ASD have difficulty processing various streams of simultaneous sensory input [see Marco et al. (4), for a review]. Indeed, neurophysiologic findings have corroborated these arguments. For instance, subjects with ASD have been shown to have deficits in processing illusions, such as the McGurk effect, which rely on integration of multiple sensory inputs (84). Findings from the current study may elucidate neurobiological underpinnings of these deficiencies in multisensory integration. For instance, the clear lack of volumetric correlation between the cerebral hemispheres may suggest that sensory cortices are not communicating with each other normally, assuming that such communication results in mutually trophic influence. Such a lack of neural connectivity could contribute to disordered multisensory integration. That is, white matter abnormalities can lead to deficiencies in processing the precise timing of action potentials, which is a prerequisite for accurate sensory processing and multisensory integration (85). One previous study showed significant correlations between behavioral measures of sensory processing and multisensory integration and white matter abnormalities, including those in the mid posterior region of the corpus callosum, in children with sensory processing disorder (85).

Cerebellum–Cortex Correlations

The difference in significant cerebellar–cortex correlations seen in the present study between the ASD and TD groups may be indicative of altered connectivity between these brain regions in the former. Decreased covariation between cerebellum and sensory cortices could be related to abnormal sensory reactivity in ASD in a number of ways. For instance, Courchesne and Allen (29) have theorized that the cerebellum monitors sensory inputs and uses them to create predictions of future events, based on past experience, and then prepares the organism to respond to these stimuli. Disruptions in this predictive ability tend to lead to deficiencies in predicting sensory events and adaptive responses to the same. Differences between predicted sensory occurrences and actual sensory input (i.e., prediction errors) could lead to sensory stimulation being perceived as strange, unpleasant, surprising, and/or overwhelming (16, 29, 86, 87). Given the cellular, structural, and functional connectivity-based abnormalities that have been reported in ASD (18, 19, 21, 79), the sensory inputs to the cerebellum, and its role in prediction, one might reason that cerebellar deficiency might plausibly be related to sensory dysfunction in ASD. Additionally, the cerebellum may play an important role in multisensory integration (24, 28), as it typically receives and sends projections from and to sensory cortices. For example, many of these projections come from the superior colliculus (SC), where, especially, auditory and visual sensory inputs are combined to form a multisensory representation of various aspects of our environment. Once information from the SC is sent to the cerebellum (particularly the vermis, lobules VI and VII), it is modulated—either enhanced or depressed—and sent back to the SC, where it is sent both to the cortex and subcortical areas. Abnormal integration or modulation of multisensory information could lead to inaccuracies or confusion in their interpretation and the responses to the same (24). Thus, it is plausible that the connectivity between the cerebellum and sensory cortices contributes a great deal to sensory processing, and that abnormalities in these connections could lead to sensory malfunction.

Amygdala–Cortex Correlation

It is reasonable to believe that sensory input perceived as threatening (i.e., hyper-reactivity) would likely be mediated, at least in part, by the amygdala (33). Zald (34) argued that the degree to which the amygdala is stimulated during a sensory event predicted the extent to which that sensory experience was considered unpleasant or threatening. Abnormalities of the amygdala have often been reported in ASD. For example, in the

VPA rat model of ASD, affected rats were shown to have overactive amygdalae (32), which lead to hyper-reactivity, decreased inhibition, and boosted synaptic plasticity. These factors were correlated with heightened behavioral fear responsivity in these animals. Consistent with animal studies, recent studies performed in humans also found ASD subjects' amygdalae and primary auditory and somatosensory cortices to be overreactive during mildly aversive sensory stimuli, when compared to controls (6). This and a related study also both showed that the BOLD responses of ASD amygdalae were positively correlated with behavioral measures of sensory over-reactivity in these individuals (6, 36). The current study showed significantly increased structural covariance between the amygdalae and right occipital and temporal cortices, which may be suggestive of hyperconnectivity similar to that reported in the aforementioned investigations. Most of the areas that showed a significantly higher degree of correlation with the amygdalae of those with ASD, vs. TD participants, seem important for facial and human body processing—e.g., inferior temporal, fusiform, and lingual gyri. Hyperconnectivity between amygdalae and such areas may contribute to the social deficits which are common in ASD [see Schultz (88), for a review].

Hemispheric Asymmetry

Hemispheric asymmetries are commonly reported in ASD, especially as they relate to cortical regions associated with language processing. Some language-related regions such as planum temporale exhibit leftward asymmetry (89, 90). In ASD, specific asymmetry findings in such structures are mixed, but consistently show asymmetry changes (91–93). For example, studies by Rojas et al. (91, 92) showed reduced planum temporale asymmetry, with the left planum temporale smaller in ASD subjects. Herbert et al. (94), however, reported increased leftward planum temporale asymmetry in boys with autism. Gage et al. (93) showed rightward asymmetries for both planum temporale and posterior superior temporal gyrus. Such variability may be due to the homogeneity of ASD and differences in sample characteristics and/or methods. The present results show larger gray matter volumes for both left and right superior temporal gyri in the ASD group, relative to controls. In addition, the left superior temporal gyri of subjects with ASD showed no indication of being larger than their right hemisphere homolog, on average, which is consistent with the aforementioned studies. Either or both of these current findings have the potential to underlie sensory abnormalities.

While asymmetries in absolute volume were not observed in the current study, a rightward asymmetry in structural covariance was noted. That is, the average of the structural correlation coefficients between hemispheres was appreciably higher in the right hemisphere. Thus, there appears to be a significant rightward asymmetry of structural covariance of sensory-related cortical structures in the current sample. This structural covariance asymmetry could be suggestive of hyperconnectivity of sensory cortices within the right hemisphere. These findings are consistent with results from a number of recent studies using functional MRI to evaluate the resting-state functional connectivity in the brains of participants with ASD (76, 80). Both of these studies noted a pattern of hyperconnectivity in the right hemisphere of these subjects vs. controls.

While no study to our knowledge has reported such a structural covariance finding in the past, there are several potential interpretations grounded in the literature that are consistent with the current hypothesis. For instance, temporal cortices of the right hemisphere have been implicated in paralinguistic and pragmatic language processing, with left hemisphere counterparts playing an important role in linguistic (e.g., syntax and semantics) portions of language. Paralinguistic elements of language are important for understanding of communicative intent, beyond the literal meaning of words and sentences. These factors might include sarcasm, emotional content, metaphors, double meanings, other non-literal language, and prosody. The integration of both the linguistic and paralinguistic parts of language is essential for accurate discourse comprehension, and, thus, to successful social functioning. Previous studies have shown that patients with right hemisphere lesions made significantly more mistakes in discourse comprehension. These errors were specifically attributable to incorrect inferences about what was being said or read, due to patients' interpretations being overly literal, which is also a common phenotype in the ASD population [see Mitchell and Crow (95), for a review]. Thus, rightward asymmetry of structural covariance may represent a dysfunction of connectivity between regions that play a role in paralinguistic processing.

Limitations and Future Directions

While the current study may provide results that are consistent with our hypothesis and previous reports of individuals with ASD, there are several limitations that we should note. First, structural covariance and functional connectivity measures are only indirectly related to each other (96). Additionally, structural connectivity is more directly measured using diffusion tensor imaging (DTI). Furthermore, volume is only one aspect of the structures investigated in the current study. Other characteristics, such as thickness, curvature, and surface area could also be assessed in future studies, since they may represent different properties of cellular organization and/or development (97–99). Therefore, the structural covariation results presented here may not have direct functional/structural connectivity implications. Future studies should endeavor to characterize the link between structural covariance and functional/structural connectivity in autism. Such a characterization could be useful clinically, as structural MRI is in many ways more conveniently collected and analyzed than fMRI or DTI, particularly with lower functioning individuals with ASD. Covariance features extracted from automated structural MRI analyses could be amenable for use with infants and young children, and other patients who otherwise could not participate in fMRI recordings.

Another weakness of the current investigation is that the data analyzed here were not specifically collected to examine sensory dysfunction in ASD. While this fact should not change the structural covariance results, it means that no behavioral data related to sensory functioning were collected alongside anatomical data. Thus, we were unable to explore any potential links between anatomical and behavioral phenomena. Several

previous studies have presented data examining relationships between structural covariance and behavior. For instance, one group has argued that various characteristics of structural covariance are useful as diagnostic predictors of patients with ASD (48). In addition, since correlation coefficients are a composite measure, we did not have values representing the strength of structural covariance for each participant. This statistical reality meant that we were unable to correlate other factors, such as age, with correlation results. Thus, future studies should continue this line of research in order to determine the association between structural covariance, behavior, and demographics, and the clinical usefulness of these neuroimaging and analysis techniques.

ETHICS STATEMENT

This study was carried out in accordance with the recommendations of the Belmont Report as reviewed by the Colorado Multiple Institutional Review Board with written informed consent from all subjects or their guardians. Additionally, all children aged seven and above provided written assent prior to participating in the study. All subjects gave written informed consent/assent in accordance with the Declaration of Helsinki. The protocol was approved by the Colorado Multiple Institutional Review Board.

AUTHOR CONTRIBUTIONS

GC and DR contributed equally to the conceptualization, hypothesis development, data analysis and interpretation, writing, and editing of the current manuscript. SH and DR worked to recruit participants and acquire behavioral and MRI data with each subject. SH also assisted in the writing and editing of the article.

FUNDING

Research funded by NIMH T32MH015442 to author GC and R01 MH082820 to author DR.

SUPPLEMENTARY MATERIAL

The Supplementary Material for this article can be found online at http://www.frontiersin.org/article/10.3389/fneur.2017.00615/full#supplementary-material.

REFERENCES

1. American Psychiatric Association. *Diagnostic and Statistical Manual of Mental Disorders: DSM-5*. Washington, DC: American Psychiatric Association (2013).
2. Baranek GT, David FJ, Poe MD, Stone WL, Watson LR. Sensory experiences questionnaire: discriminating sensory features in young children with autism, developmental delays, and typical development. *J Child Psychol Psychiatry* (2006) 47(6):591–601. doi:10.1111/j.1469-7610.2005.01546.x
3. Leekam SR, Nieto C, Libby SJ, Wing L, Gould J. Describing the sensory abnormalities of children and adults with autism. *J Autism Dev Disord* (2007) 37(5):894–910. doi:10.1007/s10803-006-0218-7
4. Marco EJ, Hinkley LBN, Hill SS, Nagarajan SS. Sensory processing in autism: a review of neurophysiologic findings. *Pediatr Res* (2011) 69:48R–54R. doi:10.1203/PDR.0b013e3182130c54
5. Tomchek SD, Huebner RA, Dunn W. Patterns of sensory processing in children with an autism spectrum disorder. *Res Autism Spectr Disord* (2014) 8(9):1214–24. doi:10.1016/j.rasd.2014.06.006
6. Green SA, Hernandez L, Tottenham N, Krasileva K, Bookheimer SY, Dapretto M. Neurobiology of sensory overresponsivity in youth with autism spectrum disorders. *JAMA Psychiatry* (2015) 72(8):778–86. doi:10.1001/jamapsychiatry.2015.0737
7. Frith U. *Autism: Explaining the Enigma*. 1st ed. Oxford, UK: Blackwell (1989).
8. Brock J, Brown CC, Boucher J, Rippon G. The temporal binding deficit hypothesis of autism. *Dev Psychopathol* (2002) 14(02):209–24. doi:10.1017/S0954579402002018
9. Rubenstein JLR, Merzenich MM. Model of autism: increased ratio of excitation/inhibition in key neural systems. *Genes Brain Behav* (2003) 2(5):255–67. doi:10.1034/j.1601-183X.2003.00037.x
10. Frith C. Is autism a disconnection disorder? *Lancet Neurol* (2004) 3(10):577. doi:10.1016/S1474-4422(04)00875-0
11. Just MA, Cherkassky VL, Keller TA, Minshew NJ. Cortical activation and synchronization during sentence comprehension in high-functioning autism: evidence of underconnectivity. *Brain* (2004) 127(8):1811–21. doi:10.1093/brain/awh199
12. Courchesne E, Pierce K. Why the frontal cortex in autism might be talking only to itself: local over-connectivity but long-distance disconnection. *Curr Opin Neurobiol* (2005) 15(2):225–30. doi:10.1016/j.conb.2005.03.001
13. Courchesne E, Pierce K. Brain overgrowth in autism during a critical time in development: implications for frontal pyramidal neuron and interneuron development and connectivity. *Int J Dev Neurosci* (2005) 23(2–3):153–70. doi:10.1016/j.ijdevneu.2005.01.003
14. Happé F. The weak central coherence account of autism. In: Volkmar FR, Paul R, Klin A, Cohen D, editors. *Handbook of Autism and Pervasive Developmental Disorders*, Vol. 1, 3rd ed. Hoboken, NJ: John Wiley & Sons, Inc (2005). p. 640–9. doi:10.1002/9780470939345.ch24
15. Geschwind DH, Levitt P. Autism spectrum disorders: developmental disconnection syndromes. *Curr Opin Neurobiol* (2007) 17(1):103–11. doi:10.1016/j.conb.2007.01.009
16. Van Boxtel JJA, Lu H. A predictive coding perspective on autism spectrum disorders. *Front Psychol* (2013) 4:19. doi:10.3389/fpsyg.2013.00019
17. Baumann O, Borra RJ, Bower JM, Cullen KE, Habas C, Ivry RB, et al. Consensus paper: the role of the cerebellum in perceptual processes. *Cerebellum* (2015) 14(2):197–220. doi:10.1007/s12311-014-0627-7
18. Ritvo ER, Freeman BJ, Scheibel AB, Duong T, Robinson H, Guthrie D, et al. Lower Purkinje cell counts in the cerebella of four autistic subjects: initial findings of the UCLA-NSAC autopsy research report. *Am J Psychiatry* (1986) 143:862–6. doi:10.1176/ajp.143.7.862
19. Kemper TL, Bauman M. Neuropathology of infantile autism. *J Neuropathol Exp Neurol* (1998) 57(7):645–52. doi:10.1097/00005072-199807000-00001
20. Courchesne E, Yeung-Courchesne R, Press GA, Hesselink JR, Jernigan TL. Hypoplasia of cerebellar vermal lobules VI and VII in autism. *N Engl J Med* (1988) 318(21):1349–54. doi:10.1056/NEJM198805263182102
21. Courchesne E. Neuroanatomic imaging in autism. *Pediatrics* (1991) 87(5):781–90.
22. Courchesne E. New evidence of cerebellar and brain stem hypoplasia in autistic infants, children, and adolescents: the MR imaging study by Hashimoto and colleagues. *J Autism Dev Disord* (1995) 25(1):19–22. doi:10.1007/BF02178164
23. Pierce K, Courchesne E. Evidence for a cerebellar role in reduced exploration and stereotyped behavior in autism. *Biol Psychiatry* (2001) 49(8):655–64. doi:10.1016/S0006-3223(00)01008-8
24. Kern JK. The possible role of the cerebellum in autism/PDD: disruption of a multisensory feedback loop. *Med Hypotheses* (2002) 59(3):255–60. doi:10.1016/S0306-9877(02)00212-8
25. Courchesne E. Brainstem, cerebellar and limbic neuroanatomical abnormalities in autism. *Current Opinion in Neurobiology* (1997) 7(2):269–78. doi:10.1016/S0959-4388(97)80016-5
26. Rojas DC, Peterson E, Winterrowd E, Reite ML, Rogers SJ, Tregellas JR. Regional gray matter volumetric changes in autism associated with

social and repetitive behavior symptoms. *BMC Psychiatry* (2006) 6:56. doi:10.1186/1471-244X-6-56
27. Kandel E, Schwartz J, Jessell T. *Principles of Neural Science*. 3rd ed. Norwalk, CT: Appleton and Lange (1991).
28. Erickson LC, Zielinski BA, Zielinski JEV, Liu G, Turkeltaub PE, Leaver AM, et al. Distinct cortical locations for integration of audiovisual speech and the McGurk effect. *Front Psychol* (2014) 5:534. doi:10.3389/fpsyg.2014.00534
29. Courchesne E, Allen G. Prediction and preparation, fundamental functions of the cerebellum. *Learn Mem* (1997) 4(1):1–35. doi:10.1101/lm.4.1.1
30. Schmahmann JD. Rediscovery of an early concept. *Int Rev Neurobiol* (1997) 41:3–27. doi:10.1016/S0074-7742(08)60345-1
31. Markram K, Markram H. The intense world theory – a unifying theory of the neurobiology of autism. *Front Hum Neurosci* (2010) 4:224. doi:10.3389/fnhum.2010.00224
32. Markram K, Rinaldi T, La Mendola D, Sandi C, Markram H. Abnormal fear conditioning and amygdala processing in an animal model of autism. *Neuropsychopharmacology* (2008) 33(4):901–12. doi:10.1038/sj.npp.1301453
33. Markram H, Rinaldi T, Markram K. The intense world syndrome – an alternative hypothesis for autism. *Front Neurosci* (2007) 1(1):77–96. doi:10.3389/neuro.01.1.1.006.2007
34. Zald DH. The human amygdala and the emotional evaluation of sensory stimuli. *Brain Res Brain Res Rev* (2003) 41(1):88–123. doi:10.1016/S0165-0173(02)00248-5
35. Green SA, Ben-Sasson A. Anxiety disorders and sensory over-responsivity in children with autism spectrum disorders: is there a causal relationship? *J Autism Dev Disord* (2010) 40(12):1495–504. doi:10.1007/s10803-010-1007-x
36. Green SA, Rudie JD, Colich NL, Wood JJ, Shirinyan D, Hernandez L, et al. Overreactive brain responses to sensory stimuli in youth with autism spectrum disorders. *J Am Acad Child Adolesc Psychiatry* (2013) 52(11):1158–72. doi:10.1016/j.jaac.2013.08.004
37. Cherkassky VL, Kana RK, Keller TA, Just MA. Functional connectivity in a baseline resting-state network in autism. *Neuroreport* (2006) 17(16):1687–90. doi:10.1097/01.wnr.0000239956.45448.4c
38. Monk CS, Peltier SJ, Wiggins JL, Weng S-J, Carrasco M, Risi S, et al. Abnormalities of intrinsic functional connectivity in autism spectrum disorders. *Neuroimage* (2009) 47(2):764–72. doi:10.1016/j.neuroimage.2009.04.069
39. Weng S-J, Wiggins JL, Peltier SJ, Carrasco M, Risi S, Lord C, et al. Alterations of resting state functional connectivity in the default network in adolescents with autism spectrum disorders. *Brain Res* (2010) 1313:202–14. doi:10.1016/j.brainres.2009.11.057
40. Hahn A, Stein P, Windischberger C, Weissenbacher A, Spindelegger C, Moser E, et al. Reduced resting-state functional connectivity between amygdala and orbitofrontal cortex in social anxiety disorder. *Neuroimage* (2011) 56(3):881–9. doi:10.1016/j.neuroimage.2011.02.064
41. Kim MJ, Loucks RA, Palmer AL, Brown AC, Solomon KM, Marchante AN, et al. The structural and functional connectivity of the amygdala: from normal emotion to pathological anxiety. *Behav Brain Res* (2011) 223(2):403–10. doi:10.1016/j.bbr.2011.04.025
42. Shin LM, Rauch SL, Pitman RK. Amygdala, medial prefrontal cortex, and hippocampal function in PTSD. *Ann N Y Acad Sci* (2006) 1071(1):67–79. doi:10.1196/annals.1364.007
43. Washington SD, Gordon EM, Brar J, Warburton S, Sawyer AT, Wolfe A, et al. Dysmaturation of the default mode network in autism. *Hum Brain Mapp* (2014) 35(4):1284–96. doi:10.1002/hbm.22252
44. Rippon G, Brock J, Brown C, Boucher J. Disordered connectivity in the autistic brain: challenges for the "new psychophysiology". *Int J Psychophysiol* (2007) 63(2):164–72. doi:10.1016/j.ijpsycho.2006.03.012
45. Pua EPK, Bowden SC, Seal ML. Autism spectrum disorders: neuroimaging findings from systematic reviews. *Res Autism Spectr Disord* (2017) 34:28–33. doi:10.1016/j.rasd.2016.11.005
46. Mechelli A, Friston KJ, Frackowiak RS, Price CJ. Structural covariance in the human cortex. *J Neurosci* (2005) 25(36):8303–10. doi:10.1523/JNEUROSCI.0357-05.2005
47. McAlonan GM, Cheung V, Cheung C, Suckling J, Lam GY, Tai KS, et al. Mapping the brain in autism. A voxel-based MRI study of volumetric differences and intercorrelations in autism. *Brain* (2005) 128(Pt 2):268–76. doi:10.1093/brain/awh332
48. Wee CY, Wang L, Shi F, Yap PT, Shen D. Diagnosis of autism spectrum disorders using regional and interregional morphological features. *Hum Brain Mapp* (2014) 35(7):3414–30. doi:10.1002/hbm.22411
49. Lord C, Risi S, Lambrecht L, Cook EH Jr, Leventhal BL, DiLavore PC, et al. The autism diagnostic observation schedule-generic: a standard measure of social and communication deficits associated with the spectrum of autism. *J Autism Dev Disord* (2000) 30(3):205–23. doi:10.1023/A:1005592401947
50. Lord C, Rutter M, Le Couteur A. Autism diagnostic interview-revised: a revised version of a diagnostic interview for caregivers of individuals with possible pervasive developmental disorders. *J Autism Dev Disord* (1994) 24(5):659–85. doi:10.1007/BF02172145
51. Rutter M, Bailey A, Lord C. *Social Communication Questionnaire (SCQ)*. Los Angeles: Western Psychological Services (2003).
52. Constantino JN, Davis S, Todd R, Schindler M, Gross M, Brophy S, et al. Validation of a brief quantitative measure of autistic traits: comparison of the social responsiveness scale with the autism diagnostic interview – revised. *J Autism Dev Disord* (2003) 33:427–33. doi:10.1023/A:1025014929212
53. Han X, Jovicich J, Salat D, van der Kouwe A, Quinn B, Czanner S, et al. Reliability of MRI-derived measurements of human cerebral cortical thickness: the effects of field strength, scanner upgrade and manufacturer. *Neuroimage* (2006) 32:180–94. doi:10.1016/j.neuroimage.2006.02.051
54. Reuter M, Schmansky NJ, Rosas HD, Fischl B. Within-subject template estimation for unbiased longitudinal image analysis. *Neuroimage* (2012) 61(4):1402–18. doi:10.1016/j.neuroimage.2012.02.084
55. Dale AM, Fischl B, Sereno MI. Cortical surface-based analysis. I. Segmentation and surface reconstruction. *Neuroimage* (1999) 9:179–94. doi:10.1006/nimg.1998.0395
56. Dale AM, Sereno MI. Improved localization of cortical activity by combining EEG and MEG with MRI cortical surface reconstruction: a linear approach. *J Cogn Neurosci* (1993) 5:162–76. doi:10.1162/jocn.1993.5.2.162
57. Fischl B, Dale AM. Measuring the thickness of the human cerebral cortex from magnetic resonance images. *Proc Natl Acad Sci U S A* (2000) 97:11050–5. doi:10.1073/pnas.200033797
58. Fischl B, Liu A, Dale AM. Automated manifold surgery: constructing geometrically accurate and topologically correct models of the human cerebral cortex. *IEEE Trans Med Imaging* (2001) 20:70–80. doi:10.1109/42.906426
59. Fischl B, Salat DH, Busa E, Albert M, Dieterich M, Haselgrove C, et al. Whole brain segmentation: automated labeling of neuroanatomical structures in the human brain. *Neuron* (2002) 33:341–55. doi:10.1016/S0896-6273(02)00569-X
60. Fischl B, Salat DH, van der Kouwe AJ, Makris N, Segonne F, Quinn BT, et al. Sequence-independent segmentation of magnetic resonance images. *Neuroimage* (2004) 23(Suppl 1):S69–84. doi:10.1016/j.neuroimage.2004.07.016
61. Fischl B, Sereno MI, Dale AM. Cortical surface-based analysis. II: inflation, flattening, and a surface-based coordinate system. *Neuroimage* (1999) 9:195–207. doi:10.1006/nimg.1998.0396
62. Fischl B, Sereno MI, Tootell RB, Dale AM. High-resolution intersubject averaging and a coordinate system for the cortical surface. *Hum Brain Mapp* (1999) 8:272–84. doi:10.1002/(SICI)1097-0193(1999)8:4<272::AID-HBM10>3.0.CO;2-4
63. Fischl B, van der Kouwe A, Destrieux C, Halgren E, Segonne F, Salat DH, et al. Automatically parcellating the human cerebral cortex. *Cereb Cortex* (2004) 14:11–22. doi:10.1093/cercor/bhg087
64. Jovicich J, Czanner S, Greve D, Haley E, van der Kouwe A, Gollub R, et al. Reliability in multi-site structural MRI studies: effects of gradient non-linearity correction on phantom and human data. *Neuroimage* (2006) 30:436–43. doi:10.1016/j.neuroimage.2005.09.046
65. Segonne F, Dale AM, Busa E, Glessner M, Salat D, Hahn HK, et al. A hybrid approach to the skull stripping problem in MRI. *Neuroimage* (2004) 22:1060–75. doi:10.1016/j.neuroimage.2004.03.032

66. Reuter M, Rosas HD, Fischl B. Highly accurate inverse consistent registration: a robust approach. *Neuroimage* (2010) 53(4):1181–96. doi:10.1016/j.neuroimage.2010.07.020
67. Tanabe J, York P, Krmpotich T, Miller D, Dalwani M, Sakai JT, et al. Insula and orbitofrontal cortical morphology in substance dependence is modulated by sex. *AJNR Am J Neuroradiol* (2013) 34(6):1150–6. doi:10.3174/ajnr.A3347
68. Desikan RS, Segonne F, Fischl B, Quinn BT, Dickerson BC, Blacker D, et al. An automated labeling system for subdividing the human cerebral cortex on MRI scans into gyral based regions of interest. *Neuroimage* (2006) 31:968–80. doi:10.1016/j.neuroimage.2006.01.021
69. Buckner RL, Krienen FM, Castellanos A, Diaz JC, Yeo BTT. The organization of the human cerebellum estimated by intrinsic functional connectivity. *J Neurophysiol* (2011) 106(5):2322–45. doi:10.1152/jn.00339.2011
70. Yeo BTT, Krienen FM, Sepulcre J, Sabuncu MR, Lashkari D, Hollinshead M, et al. The organization of the human cerebral cortex estimated by intrinsic functional connectivity. *J Neurophysiol* (2011) 106(3):1125–65. doi:10.1152/jn.00338.2011
71. IBM Corp. *IBM SPSS Statistics for Windows*. Version 23.0. Armonk, NY: IBM Corp (2014).
72. Yekutieli D, Benjamini Y. Resampling-based false discovery rate controlling multiple test procedures for correlated test statistics. *J Stat Plan Inference* (1999) 82(1–2):171–96. doi:10.1016/S0378-3758(99)00041-5
73. Cohen J, Cohen P. Applied multiple regression/correlation analysis for the behavioral sciences. Hillsdale, NJ: Erlbaum (1983).
74. Paakki J-J, Rahko J, Long X, Moilanen I, Tervonen O, Nikkinen J, et al. Alterations in regional homogeneity of resting-state brain activity in autism spectrum disorders. *Brain Res* (2010) 1321:169–79. doi:10.1016/j.brainres.2009.12.081
75. Anderson JS, Nielsen JA, Froehlich AL, DuBray MB, Druzgal TJ, Cariello AN, et al. Functional connectivity magnetic resonance imaging classification of autism. *Brain* (2011) 134(12):3742–54. doi:10.1093/brain/awr263
76. Maximo JO, Keown CL, Nair A, Müller R-A. Approaches to local connectivity in autism using resting state functional connectivity MRI. *Front Hum Neurosci* (2013) 7:605. doi:10.3389/fnhum.2013.00605
77. Rudie JD, Dapretto M. Convergent evidence of brain overconnectivity in children with autism? *Cell Rep* (2013) 5(3):565–6. doi:10.1016/j.celrep.2013.10.043
78. Hull JV, Jacokes ZJ, Torgerson CM, Irimia A, Van Horn JD. Resting-state functional connectivity in autism spectrum disorders: a review. *Front Psychiatry* (2017) 7:205. doi:10.3389/fpsyt.2016.00205
79. Olivito G, Clausi S, Laghi F, Tedesco AM, Baiocco R, Mastropasqua C, et al. Resting-state functional connectivity changes between dentate nucleus and cortical social brain regions in autism spectrum disorders. *Cerebellum* (2017) 16(2):283–92. doi:10.1007/s12311-016-0795-8
80. Cardinale RC, Shih P, Fishman I, Ford LM, Müller R-A. Pervasive rightward asymmetry shifts of functional networks in autism spectrum disorder. *JAMA Psychiatry* (2013) 70(9):975–82. doi:10.1001/jamapsychiatry.2013.382
81. Hirstein W, Iversen P, Ramachandran VS. Autonomic responses of autistic children to people and objects. *Proc R Soc Lond B Biol Sci* (2001) 268:1883–8. doi:10.1098/rspb.2001.1724
82. Schoen SA, Miller LJ, Brett-Green B, Hepburn SL. Psychophysiology of children with autism spectrum disorder. *Res Autism Spectr Disord* (2008) 2(3):417–29. doi:10.1016/j.rasd.2007.09.002
83. Lane SJ, Reynolds S, Dumenci L. Sensory overresponsivity and anxiety in typically developing children and children with autism and attention deficit hyperactivity disorder: cause or coexistence? *Am J Occup Ther* (2012) 66(5):595–603. doi:10.5014/ajot.2012.004523
84. Bebko JM, Schroeder JH, Weiss JA. The McGurk effect in children with autism and Asperger syndrome. *Autism Res* (2014) 7(1):50–9. doi:10.1002/aur.1343
85. Owen JP, Marco EJ, Desai S, Fourie E, Harris J, Hill SS, et al. Abnormal white matter microstructure in children with sensory processing disorders. *Neuroimage Clin* (2013) 2:844–53. doi:10.1016/j.nicl.2013.06.009
86. Pellicano E. Sensory symptoms in autism: a blooming, buzzing confusion? *Child Dev Perspect* (2013) 7(3):143–8. doi:10.1111/cdep.12031
87. Sinha P, Kjelgaard MM, Gandhi TK, Tsourides K, Cardinaux AL, Pantazis D, et al. Autism as a disorder of prediction. *Proc Natl Acad Sci U S A* (2014) 111(42):15220–5. doi:10.1073/pnas.1416797111
88. Schultz RT. Developmental deficits in social perception in autism: the role of the amygdala and fusiform face area. *Int J Dev Neurosci* (2005) 23(2–3):125–41. doi:10.1016/j.ijdevneu.2004.12.012
89. Kulynych JJ, Vladar K, Jones DW, Weinberger DR. Gender differences in the normal lateralization of the supra-temporal cortex: MRI surface rendering morphometry of Heschl's gyrus and the planum temporale. *Cereb Cortex* (1994) 4:107–18. doi:10.1093/cercor/4.2.107
90. Preis S, Jancke L, Schmitz-Hillebrecht J, Steinmetz H. Child age and planum temporale asymmetry. *Brain Cogn* (1999) 40(3):441–52. doi:10.1006/brcg.1998.1072
91. Rojas DC, Bawn SD, Benkers TL, Reite ML, Rogers SJ. Smaller left hemisphere planum temporale in adults with autistic disorder. *Neurosci Lett* (2002) 328(3):237–40. doi:10.1016/S0304-3940(02)00521-9
92. Rojas DC, Camou SL, Reite ML, Rogers SJ. Planum temporale volume in children and adolescents with autism. *J Autism Dev Disord* (2005) 35(4):479–86. doi:10.1007/s10803-005-5038-7
93. Gage NM, Juranek J, Filipek PA, Osann K, Flodman P, Isenberg AL, et al. Rightward hemispheric asymmetries in auditory language cortex in children with autistic disorder: an MRI investigation. *J Neurodev Disord* (2009) 1(3):205–14. doi:10.1007/s11689-009-9010-2
94. Herbert MR, Ziegler DA, Deutsch CK, O'Brien LM, Kennedy DN, Filipek PA, et al. Brain asymmetries in autism and developmental language disorder: a nested whole-brain analysis. *Brain* (2005) 128:213–26. doi:10.1093/brain/awh330
95. Mitchell RLC, Crow TJ. Right hemisphere language functions and schizophrenia: the forgotten hemisphere? *Brain* (2005) 128(5):963–78. doi:10.1093/brain/awh466
96. Honey CJ, Sporns O, Cammoun L, Gigandet X, Thiran JP, Meuli R, et al. Predicting human resting-state functional connectivity from structural connectivity. *PNAS* (2009) 106:2035–40. doi:10.1073/pnas.0811168106
97. Rakic P. Defects of neuronal migration and the pathogenesis of cortical malformations. *Prog Brain Res* (1988) 73:15–37. doi:10.1016/S0079-6123(08)60494-X
98. Balardin JB, Comfort WE, Daly E, Murphy C, Andrews D, Murphy DGM, et al. Decreased centrality of cortical volume covariance networks in autism spectrum disorders. *J Psychiatr Res* (2015) 69:142–9. doi:10.1016/j.jpsychires.2015.08.003
99. Eisenberg IW, Wallace GL, Kenworthy L, Gotts SJ, Martin A. Insistence on sameness relates to increased covariance of gray matter structure in autism spectrum disorder. *Mol Autism* (2015) 6(1):54. doi:10.1186/s13229-015-0047-7

Conflict of Interest Statement: The authors declare that the research was conducted in the absence of any commercial or financial relationships that could be construed as a potential conflict of interest.

Copyright © 2017 Cardon, Hepburn and Rojas. This is an open-access article distributed under the terms of the Creative Commons Attribution License (CC BY). The use, distribution or reproduction in other forums is permitted, provided the original author(s) or licensor are credited and that the original publication in this journal is cited, in accordance with accepted academic practice. No use, distribution or reproduction is permitted which does not comply with these terms.